STUDIES IN THE MEASUREMENT OF NUCLEAR RADIATIONS OF EXTREMELY LOW INTENSITY — CARBON-14 DATING

Thesis by

Norman Ford Jacobson

In Partial Fulfillment of the Requirements

For the Degree of

Doctor of Philosophy

California Institute of Technology

Pasadena, California

1956

FRONT PIECE

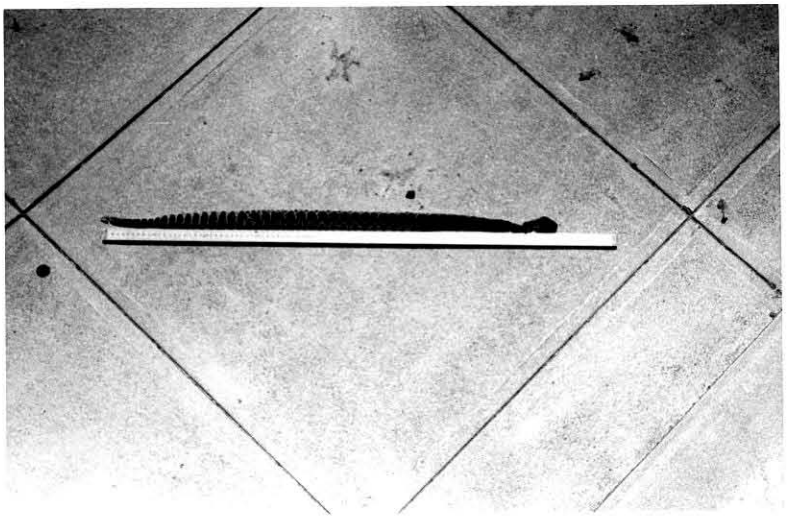

Photograph No. 1 This rattlesnake was encountered and killed near the entrance to the 937 ft. gallery at Morris Dam.

Photograph No. 2 The above snake was encountered on this path approximately at the point of the shadow. This path leads to the entrance of the 937 ft. gallery.

ACKNOWLEDGEMENTS

In my course of study and research at the California Institute of Technology, many, many people have given of their time and effort in my behalf. It is only proper that I indicate my appreciation for their consideration at this time; however, the number of persons involved makes it impossible for me to include all their names here. Nevertheless, I would like to express my special appreciation to Professor Don M. Yost, Professor N. Victor Neher and Professor Robert F. Bacher, who played major roles in guiding this work. I would also like to acknowledge the aid of Mr. Fred Chapman and the Metropolitan Water District of Pasadena for the use of their facilities at Morris Dam near Azusa, California; and Mr. Peter Nahl and the Riverside Cement Company for the use of the facilities at their Riverside Mine near Riverside, California. I would like to thank Mr. Philip Orr and the Santa Barbara Museum of Natural History for the archeological samples from the Santa Rosa Islands which they supplied; Professor Edmund Shuleman for the Sequoia Gigantea redwood sample which he supplied; the Eastman Kodak Company for the financial aid of their fellowship, and finally, the Physics and Chemistry departments of the California Institute of Technology and their personnel for their general assistance. To all persons whose aid I received, may I express my sincere appreciation.

NORMAN F. JACOBSON

The research described in this thesis was carried out under the auspices of the Atomic Energy Commission.

ABSTRACT

The technical details of a radiation measuring system based on a quartz torsion fiber electroscope and a pressurized ionization chamber are described. This equipment is designed to measure the radiation intensity from the carbon-14 contained in a sample introduced into the system as carbon dioxide. This system, including the shielding, is shown to be capable of measuring nuclear radiations of extremely low intensities, on the order of 1/200 of the normal laboratory background level, with a probable error of approximately 1%. The background radiation intensity observed with the system including the shielding is also on the order of 1/200 of the normal laboratory background level. The nature of background radiation and its relation to the measurement of such low intensities is discussed. It is shown that the main limitation in accuracy, with the equipment described here, is due to cosmic ray bursts. It is also shown that the major source of background radiation is external to the equipment, being thus due to cosmic rays and/or local external gamma ray emitting material contamination. Although the evidence is not conclusive, the data indicates in addition that the cosmic rays are the major contributor to this background radiation. The main conclusion which may be drawn from these results is that the selection of an equipment location is very effective in reducing the level of background radiation, thus permitting the measurement of radiation fields of extremely low intensity. The final application of this equipment was to the well known carbon-14 dating method originated by W. F. Libby. Several samples of interest were dated and the results are given. Of particular interest, are the samples from the Santa Rosa Islands off the California Coast, concerning an Indian culture which existed there before Christ and after.

TABLE OF CONTENTS

TABLE OF CONTENTS (Cont'd)

Introduction:

During the last decade since its discovery in 1946, the now well known carbon-14 dating method has been undergoing the usual development in experimental technique. The work which will be described in this thesis is a part of this development.

Historical Background:

In 1934, A. V. Grosse (1) proposed the existence of "cosmic radio-elements", nuclides produced by the interactions of cosmic rays with the earth and its atmosphere. The possibility of the presence of carbon-14 in nature was first considered by S. A. Korff (2) in 1940. From nuclear physical data, W. F. Libby (3) in 1946 concluded that the neutrons in the upper atmosphere should produce carbon-14 in significant quantities. These neutrons in the upper atmosphere are the product of the primary cosmic rays' interactions with the atmosphere. The radiocarbon producing reaction considered by Libby was the following:

$$N^{14} + n \longrightarrow C^{14} + p$$

Libby also suggested that this carbon-14 might be detectable in living matter and in other forms of carbon in exchange equilibrium with atmospheric carbon dioxide, which is presumed to contain the radiocarbon. In the following year, 1947, the work of A. V. Grosse, W. F. Libby, C. E. Anderson and coworkers (4, 5) was published describing the positive results which they obtained in attempting to check Libby's hypothesis. Some of the many implications of their positive results were also discussed; and in particular, the basic

dating hypothesis was set forth. The work of Libby and his associates, as well as others, has since put the carbon-14 dating method on a rather satisfactory scientific foundation and the experimental techniques on a good practical foundation.

At this time, for the sake of completeness and clarity, the basic premises and conclusions supporting the carbon-14 dating method will be stated. They will be listed in logical order and follow below:

1. Cosmic rays have been essentially constant in type and intensity during the last 30,000 years or more. (This premise is difficult to verify except insofar as the consistent results of the entire method support it.)

2. Cosmic rays produce neutrons in the upper atmosphere through nuclear interactions. (The cosmic ray source of neutrons is the only satisfactory one consistent with their observed presence and the 20 min. half-life of the neutron.)

3. Neutrons are produced continuously and uniformly by this cosmic source. (This is the logical conclusion of statements 1 and 2.)

4. These "cosmic neutrons" enter into the nuclear reaction N-14(n, p)C-14 producing carbon-14 at a uniform rate. (The nuclear reaction has been demonstrated in the laboratory, and the uniform rate of production is a consequence of statement 3.)

5. The radiocarbon is shortly oxidized to carbon dioxide and enters into exchange equilibrium with the carbon

reservoir of the biosphere. (This statement is supported by the detection of radiocarbon in atmospheric carbon dioxide from all parts of the biosphere.)

6. Radiocarbon, as the name implies, is a radioactive isotope of carbon decaying by beta disintegration according to the usual exponential decay law. (Radiocarbon has been produced artificially in the laboratory and shown to be radioactive with a half-life of approximately 5560 years.)

7. The production process has been going on for such a time that equilibrium has been established between the uniform production process and the exponential decay process. (This idea is directly related to statement 1 and is, indeed, logically equivalent. As with statement 1, this statement is supported by the consistent results of the entire carbon-14 dating method.)

8. The time scale of mixing within the carbon reservoir is short compared to the average life-time of a carbon-14 atom thus establishing a uniform concentration of radiocarbon within the reservoir. (This statement is supported by the experimental fact that measurements on numerous samples from different locations in the reservoir do not indicate significant variations in radiocarbon concentration.)

9. Any portion of the reservoir which is separated from the remainder of the reservoir may, under certain circumstances, no longer absorb radiocarbon; however, the radiocarbon within this portion will continue to decay. Consequently, if these circumstances do exist, the

concentration of carbon-14 in this sample will decrease with time according to the exponential decay law. (This statement is in consequence of the previous statements.)

10. Under certain circumstances, the radiocarbon of the sample can be accurately measured. (This statement is simply an acknowledgement of the success of the work of Libby and others.)

11. From the magnitude of the radiocarbon concentration in any given sample and that of a normal modern sample, a sample in equilibrium with the reservoir, the time which has elapsed since the given sample was separated from the reservoir can be calculated. (This statement is the logical consequence of statements 9 and 10.)

The above eleven statements explicitly outline the basic ideas underlying the carbon-14 dating method. There are, indeed, many if's, and's and but's involved in making significant conclusions concerning any particular sample; nevertheless, the method is extremely powerful.

Technical Background:

The work described in this thesis concerns the experimental problem of determining the radiocarbon concentration of a sample. In all cases,this is done by measuring secondary effects produced by the nuclear radiations from the radioactive carbon-14. The following is a technical background covering the basic measurement problem and the methods of solution.

Carbon-14 is a radioactive isotope of carbon decaying by means of beta disintegration; the maximum beta energy is 155 kev., and the average beta energy is approximately 47 kev. The specific activity of natural carbon in exchange equilibrium with the cosmic radiocarbon is approximately 15 disintegrations per minute per gram of carbon. This specific activity represents a mass ratio of carbon-14 to carbon-12 of approximately 1 to 10^{12}. Normal laboratory background radiation produces approximately 10 ion pairs per second per cubic centimeter in air at S. T. P. The radioactivity from the carbon-14 contained in 1 cubic centimeter of pure carbon dioxide at S. T. P. and in exchange equilibrium with the carbon reservoir will produce only 0.2 ion pairs per second. If one wishes to extend the dating method back 40,000 years or 7 carbon-14 half-lives, one must measure a radiation intensity producing in 1 cubic centimeter of gas under similar conditions only 0.0016 ion pairs per second, an intensity of 1/2000 of the normal background radiation intensity. These figures are not entirely representative because it depends somewhat on the sensitivity of the radiation detecting device; nevertheless, the order of magnitude remains the same. Therefore, the problem is one of accurately measuring the intensity of a soft beta ray flux of very low intensity.

Libby and his associates (6) solved this experimental problem with a, so-called, grid-walled geiger counter in conjunction with anticoincidence and material shielding. Kulp (7) and others (8, 9, 10, 11) have improved and modified Libby's basic technique. Fergusson (12) has developed a system using a proportional

counting tube as a substitute for the geiger counter. This allows him also to measure pulse sizes as well as occurrences, permitting limited pulse height discrimination. His results have been very good and represent the best to date. Arnold (13) has been attempting to develop a scintillation counting system whose advantages should be great; to date he has been successful in part.

The work to be described here concerns the application of the ionization chamber and quartz electroscope to the solution of this problem. The application of such equipment to the solution of this problem was first suggested by Professor H. V. Neher of the California Institute of Technology. The main advantage of this type of equipment is that it permits the use of a large gaseous sample. The final equipment described here was designed to hold a sample of purified carbon dioxide amounting to roughly one mole of gas within the sensitive volume of the system. A second advantage of this type of equipment is its extreme simplicity and freedom from critical operating conditions.

The Equipment:

The equipment described here may be divided into four basic parts which are:

1. Electroscope system
2. Electroscope charging and recording system
3. Ionization chamber
4. External shielding

In the succeeding sections, these basic parts of the equipment will be described in detail and their relationship to the measurement problem will be explained.

1. The Electroscope:

The electroscope system used in this equipment was constructed by the author in its entirety. The quartz fiber manipulation techniques required for this work were learned under the instruction of Professor Neher, and the equipment used was that maintained by Professor Neher in the Norman Bridge Laboratories of Physics at the California Institute of Technology. A description of these techniques and the equipment required is given in Chapter V of Strong's "Procedures in Experimental Physics" (14). This chapter was written by Professor Neher and describes the actual equipment essentially as it now appears in the Norman Bridge Laboratories.

The electroscope is a fused quartz torsion fiber type fashioned after the design of Professor Neher with a single modification. Figure 1 illustrated the physical appearance of the system. It has been found that in a system such as this in which the chamber's gaseous contents are repeatedly removed and replaced the electroscope is subjected to rather severe directional gas currents. Quite often the indicating fiber would be displaced in one direction or the other to such an extent that it could not be returned to the normal operating position without opening the chamber. The single modification in design consists, therefore, of mechanical stops which prevent such occurrences. The torsion fiber on the system used here has a diameter of 3-4 microns and the indicating fiber has a diameter of 15-20 microns. The entire system is gold plated by evaporation technique except for a small portion just

below the platinum contact. The platinum contact acts as a wear resistant contact point for the recharging rod and the unplated portion of the quartz supporting beam acts as the electroscope insulation. The gold plating is generally from 100 to 200 Angstroms thick; this is a good conducting surface coating.

Besides the above described superficial design details of the electroscope, there are several less apparent but very important specifications that must be met. The first involves the balancing of the indicating fiber. If the electroscope system is to be independent of orientation, the indicating fiber must be balanced. This is done by cutting the ends off of the indicating fiber in 1/1000 inch increments with alternate testing in a trial and error method until balance is achieved.

The next requirement is that the system have a suppressed zero so that a sufficiently large potential will be required for initial deflection of the indicating fiber; this large initial deflection potential is required to establish an adequate collection voltage gradient within the ionization chamber's sensitive volume. In construction, this is accomplished by rotating the indicating fiber one or more turns in the reverse direction and thus placing a twist in the torsion fiber; this is a very delicate operation and is done after the system is entirely constructed. The electroscope used here has one twist in its torsion fiber and requires a potential of approximately 150 volts for initial deflection.

The third important detail concerns the insulation. Quartz is probably the best insulation material known; however, this is

true only if the surface is clean. In construction of the electroscope system, one must take care not to touch the quartz unnecessarily with fingers or tools, particularly the portion destined to be the electroscope insulator. As a final step after the electroscope is complete and about to be placed within the ionization chamber, the insulating portion of the quartz must be cleaned by firing with a hot gas flame. This operation is rather touchy and must be performed with great care. The quartz must be heated hot enough, but not too hot. The hot flame must be kept away from the delicate portions of the system, and yet, all surfaces of the insulating portion must be heated. Needless to say, many a potentially excellent electroscope constructed by this author has come to a premature and disheartening end at this point.

When completed, an electroscope of the above design is a very beautiful thing, and considering its technical specifications, it is indeed noteworthy. The system has a current sensitivity on the order of 10^{-11} coulombs per millimeter which may be increased by means of optical magnification. With the quartz insulation in proper condition a very small leakage rate may be obtained. With the system used in this equipment, less than 0.01 millimeters deflection was observed over a period of 24 hours; this represents a leakage current of less than 100 electrons per second or an insulation resistance of greater than 10^{19} ohms.

Considering at this point the fused quartz used in the construction of this electroscope, the many desirable properties of the quartz should be noted. Quartz is superior to all materials in

regard to the following properties:

1. Thermal expansion and contraction
2. Elasticity
3. Thermal hysteresis
4. Mechanical hysteresis
5. Internal viscosity
6. Volume and surface resistivity
7. The ease with which it may be drawn into fibers.

Considering the physical form that the electroscope design takes as seen in figure 1, an explanation is perhaps in order. This design, as already indicated, was worked out by Professor Neher. According to him, the unexplained appendages are electrostatic shields which so shape the electric field that the electroscope discharge is essentially linear over a relatively large deflection. As verification of this fact, graphs 1 and 2 illustrate experimental data obtained with this electroscope exhibiting a high degree of linearity. Graph 1 represents point data taken on three separate discharges of the system. The other graph is actually the outline of the enlargement of a single rapid discharge trace as recorded on photographic film. Note that the enlargement is anisotropic and that the time marking lines are 10 minutes apart in time. Actually, these graphs represent an electroscope deflection of only about 1 millimeter; nevertheless, the linearity is quite good. In all future considerations, the response of the electroscope is assumed to be linear.

2. Electroscope Charging and Recording System:

This type of electroscope in operation is charged by an electric potential, and its rate of discharge is observed. When incorporated in automatic equipment, such as described here, a means of periodically recharging the electroscope is required as well as a method of recording the discharge rate. In photograph 24 a mock-up of a preliminary system is shown. Although the final system differed in certain details, it gives a clear picture of the electromagnetically operated mechanical recharging arm used in the final equipment. This arm when activated reaches out and touches the electroscope on its platinum contact; the arm is connected to batteries so that it charges the electroscope to approximately 150 volts. The schematic for the recharging cycle timing device is shown in figure 3. This device activates the recharging mechanism once every 3 1/3 hours. Note that a push-button permitting manual recharging of the system and a potentiometer permitting control of the force with which the recharging arm strikes the electroscope are provided.

In order to obtain numerical data from such an electroscope, its discharge rate must be measured; this may be done visually with perhaps the aid of a micrometer telescope. However, with this equipment where a continuous record over an extended period is required, it is done with the aid of a camera. As shown in figure 2, which illustrates the physical arrangement of the ionization chamber, electroscope and optical system, the electroscope is mounted in front of the camera lens. The indicating fiber is illuminated from below by means of a light located outside of the system. The light

enters through a window in the chamber lid and reflects off of a reflector located on the bottom of the chamber. The lens focuses the indicating fiber image onto the film in the camera; the image appears as a dark line perpendicular to the motion of travel of the indicating fiber on a light background. In order to obtain a time measurement, a slit is placed just in front of the film and behind the lens, and is positioned parallel to the direction of travel of the indicating fiber. The film is placed on a drum which rotates slowly passing the film over the slit; the film moves perpendicular to the slit and the motion of travel of the indicating fiber. The result of this arrangement is a diagonal line representing a deflection versus time plot of the electroscope discharge. With the equipment described here the film drum rotates approximately once every 40 hours.

It was found very difficult to build a gear train which would give the drum a constant uniform motion; in fact, it was found that the final system had a major periodic variation of approximately 10% in rate and a period of approximately one hour in addition to minor variations. In order to overcome such difficulties, it was found satisfactory to determine the time scale precisely at periodic intervals. This was accomplished in the following manner: A 1/10 rpm synchronous motor was connected directly to a cam mechanism which closes a microswitch every 10 minutes. The closure is estimated to be accurate to better than 0.1% in 10 minutes. The microswitch contacts turn on a light located below and to one side of the optical slit, and a thermal delay relay allows the light to remain on for 2 seconds. The result of this arrangement is an

image of the slit appearing on the film precisely every 10 minutes. With this system, a precise time measurement is provided as well as a continuous record of the electroscope discharge. It was found necessary to use the very fast Tri-X film in the camera so that a small slit could be used to insure good resolution of the discharge variations and at the same time to allow the use of a small size illuminating light. The slit used in this equipment is 40 micron wide, and the film passes across the slit in 20 seconds. It has been found that too large a light source permits too much infra-red radiation to enter the chamber producing convection currents within the filling gas which can disturb the electroscope. In one system, the electroscope was entirely inoperative due to this effect. In addition to the fast film, it was found necessary to use a relatively fast lens (f-2.7) and an optically adequate illuminating system to obtain a good image of the indicating fiber and sufficient light to expose the film adequately. Photograph 25 shows the camera with its lid off revealing the film drum with a strip of Tri-X Eastman Kodak 35 mm. film in place. Figure 4 gives the schematic of the time marking device. Figures 5 and 6 give the electrical schematic for the camera power supply and the light source power supply respectively. Photographs 14 and 15 give views of the actual equipment as it appeared preparatory to being put into operation.

3. Ionization Chamber:

The ionization chamber into which this electroscope and optical system is built is constructed of steel which will withstand pressures of several hundred pounds per square inch. The shape

is cylindrical with a diameter of 16 cm. and a height of 22 cm.; the volume is approximately 3.7 liters. Inside of this container, a cylindrical grid-like structure is mounted. The grid is made of 3 mil iron wire spaced 1/4" apart and is supported on a steel frame with the approximate dimensions of diameter 13 cm. and height 16.5 cm. The iron wires cut off an effective volume of 2.3 liters within the chamber. This so-called grid wall is electrically insulated from the walls of the steel container and maintained at a potential different than the steel container. The function of this grid wall will be discussed later. In order to allow light to enter and leave the system, two windows are located in the chamber lid. The windows are made of $\frac{1}{2}$" plate glass which has been ground to a conical shape. They are placed in matching conical holes in the $\frac{1}{2}$" thick, steel lid and are sealed to the steel by means of a high vacuum wax (Apiezon W). In order to prevent the wax from cold flowing out of the joint and thus allowing the glass to rest on the steel which causes the window to break, the glass is cushioned on two layers of wax impregnated filter paper. After installation, the directional pressure forces any excess wax out of the joint, and the glass rests firmly on the steel through the cushioning filter paper. The window is also supported from within the chamber by means of a collar screwed to the lid. This is required so that the system may be evacuated for extended periods of time without fear of the windows imploding. The other parts that are required to communicate through the chamber wall are mounted on the chamber lid and, in addition to mechanical support, are soft soldered to insure a vacuum seal. Photograph 24 illustrates

the construction of the grid structure, although some of the other details in the picture are not as they appear in the final equipment. Note the teflon spacers and supporting posts which insulate the grid structure from the surrounding chamber walls. Note also the electrical connections to the feed-through insulators. The recharging arm mechanism can also be seen in this photograph, and its relation to the grid structure noted. The arrangement is so designed that the entire recharging arm and mechanism is entirely outside of the grid structure when not in use. When in operation, the recharge arm passes between the wires of the grid structure in making contact with the electroscope.

Photograph 14 shows a clear view of the chamber lid and its major parts. The optical tube is seen protruding from the center with the camera mounted on one end. To the left, a pressure gage is seen; to the rear just behind the optical tube, the light source is seen; to the right, the junction box which is mounted on top of the recharging arm activating solenoid is seen, and to the front, the high pressure valve is seen. In addition to the two windows which cannot be seen, two feed-through Kovar insulators are mounted on and through the lid. One feed-through insulator supplies operating potential to the grid structure, and the other the recharging potential to the recharge arm when required.

The entire instrument, chamber, electroscope and photographic recording system, is powered and controlled by two separate electrically connected units. These two units are pictured in photograph 14. The unit on the right is the time marking

device whose function was explained under the description of the electroscope charging and recording system. The electrical schematic is shown in figure 4. The unit on the left contains 4 separate units. They are the recharging cycle timing device, the camera power supply, the light source power supply, and the batteries which supply the recharging and grid potentials. Note that all units have an associated neon indicating light so that one may be sure that all units are in operation at a glance.

4. External Shielding

The final basic part of the complete system consists of external shielding. This shielding in turn consists of two distinct parts:

1. A lead house with a top thickness of 8 inches and sides and bottom thickness of 4 inches.

2. An underground measurement location permitting a material layer overhead of 200 or more meters-water-equivalent.

The details and relation of this shielding to the measurement problem will be discussed shortly. At present, however, some preliminary subjects important to the understanding of these details will be discussed.

Statistics:

To use this equipment properly, it is necessary to understand the basic statistics which underly radioactive disintegration. Radioactivity is a nuclear phenomenon, and contrary to chemical phenomena, it is entirely independent of normal physical conditions. Each radioactive nuclei disintegrates entirely at random

with a definite probability of disintegration per unit time. As with any random event occurring in relatively small numbers, there is a certain inherent irregularity in their rate of occurrence. Over a sufficiently long period, these irregularities will average out since basically there is some unique average rate at which any given large group of a particular type of radioactive atom must decay. In measuring a radiocarbon sample, sufficient time must be allowed for the measurement consistent with the sample size and the accuracy with which the measurement must be made. However, the exact nature of the sensing and measuring device also influences the statistics. Although, under certain circumstances, there may exist a unique average rate of decay and a certain inherent variation in the average rate of decay of small samples, the product of this radioactive decay, the radiation, and the method of its detection may also have random irregularities associated with it. Since the decay rate is determined from measurements of the intensity of the radiation, these additional statistical irregularities must be included in the final analyses of the situation. In the case of geiger counters such as used by Libby, a discharge of the geiger tube indicates the presence in the sensitive volume of the geiger tube of a source of one or more free electrons. If the only source of ionizing radiation and free electrons is carbon-14, each discharge can be interpreted as due to the disintegration of a carbon-14 atom. In such a case, only the random variations of the radioactive decay process would be involved. In the case of an ionization chamber, however, individual occurrences are

not distinguished; but on the contrary, the total amount of electrical charge in the form of positive and negative ions produced in the sensitive volume of the system by the ionizing radiation is detected and measured. In the case of carbon-14 which is a soft beta emitter, each beta particle in dissipating its energy in collisions with the gas molecules produces free electrons and positive ions. The electrons may become attached to neutral atoms producing negative ions; but regardless of this, in a well designed system essentially all of these ions and/or electrons are separated and collected on the electroscope or chamber wall under the influence of the collection potential thus discharging the electroscope. A beta active substance emits a continuous energy spectrum of beta-rays, and each beta-ray produces a different number of ions in its random travel through the gas. The result is that two additional statistical quantities enter into the determination of the magnitude of the ions current ultimately produced by the radioactivity. In the case of the effect of the beta ray spectrum, it can be shown that this source of error will produce a statistical error which will increase the error of the measurement by approximately 20-25% (see Appendix) as compared to that due to the decay process only. Since the standard deviation in such a measurement is proportional to the square root of the magnitude of the ion current and the measurement time, the sample size must be increased by a factor of 1.5, or the time of measurement must be increased by a factor of 1.5 to obtain an equivalent statistical error.

In the case of an individual beta ray and its random travel

through the filling gas of the chamber, an average beta ray of 47 kev will produce approximately 1500 ion pairs with a probable variation in number of roughly 1% (15). This statistical fluctuation will also be superimposed onto the statistical fluctuation due to the decay process. Obviously under certain circumstances, this source of error must be included in the final analysis.

Background Radiation:

The above considerations have been made assuming that no background radiation is present; this, as already indicated, is not the case. Background radiation exists everywhere and represents the source of the major problem in most low level radiation measurements regardless of the type of device used. At this point, the nature of the background radiation encountered will be considered in detail. Background radiation can be grouped into the following two classifications:

1. Radioactive contamination
2. Cosmic rays

Radioactive contamination refers to radioactive materials in the local area whose radiations may reach the sensitive volume of the sensing element of the radiation detecting system. This source of background radiation may be further classified into external and internal contamination. Numerous materials external to the system contain minute quantities of uranium, thorium, their daughter products and other naturally occurring radio elements. These substances emit alpha, beta and gamma radiation which can affect the equipment; these substances are external

contamination. With this particular equipment, the only type of radiation from this source which can enter the sensitive volume of the system is the gamma radiation. There are two practical methods of reducing the level of this sort of background radiation; they are:

1. A location for operation of the equipment can be chosen which is superior in this respect to other locations.

2. Purified materials, which are relatively free from these radioactive contaminants, may be used to separate the equipment from the source of this sort of contamination. It is intended that this material will absorb part of the gamma radiation before it reaches the sensitive volume of the system without contributing additional contamination to the locality. Since elements of high atomic number absorb gamma radiation best and are also usually of high specific gravity, materials such as lead, mercury and iron are commonly used for this purpose.

Internal contamination refers to radioactive materials actually included in and on the construction materials of the equipment; internal contamination represents a somewhat more difficult problem; in this case, all three types of radiation, alpha, beta and gamma, can enter the sensitive volume of the system. Alpha radiation in passing through matter dissipates its energy very rapidly. A typical alpha particle may have a range not greater than 10 to 15 centimeters in air at S. T. P.; however, the energies of typical alpha particles from natural sources are several mev. Consequently, alpha particles cannot originate from far below

the surfaces exposed to the sensitive volume of the system; but if one does reach the sensitive volume, it dissipates its energy rapidly giving a large effective background signal. Beta radiation is intermediate between alpha and gamma radiation in penetrating power; and correspondingly, its rate of energy dissipation is also intermediate. Typical naturally occurring beta rays have energies from 50 kev and less to 3 mev and ranges of from 10 centimeters to 10 meters in air at S. T. P. Thus beta radiation can come from considerably deeper within the construction material; although when beta radiation reaches the sensitive volume, the effective background signal is not as large as with alpha radiation. In the case of internal gamma ray background radiation, the situation is essentially equivalent to external gamma radiation in effect; however, the situation with respect to its reduction and elimination is considerably different. The alpha, beta and gamma radiations described above all come from radioactive contaminating substances in or on the surfaces of the construction materials. The practical approaches to the reduction of this sort of background radiation are as follows:

1. Construction materials can be selected which are relatively free of such contaminants.

2. The proper care and treatment of the surfaces of the construction materials exposed to the sensitive volume of the system can reduce surface contaminants.

3. As with external contamination, the use of material shielding can reduce the amount of such radiation reaching the sensitive volume of the system.

However, only the alpha and beta radiations can be effectively reduced by this method. Gamma radiation cannot be greatly reduced by this approach simply because it is entirely impractical to use the thicknesses of material that are required for significant reduction.

Cosmic rays and radiation of a secondary nature produced by the cosmic rays' interactions with the earth and atmosphere constitute the other source of background radiation. At and near the surface of the earth, this radiation takes the form of very high energy mu-mesons which have very high penetrating powers being detectable at great depth under the earth and which have an energy dissipation rate roughly equal to that of a beta particle. These mesons produce two distinct types of effects in dissipating their energy in any absorbing material; the first is the production of so-called cosmic ray bursts in which the tremendous energy of a single mu-meson is converted into a dense cloud of ionizing radiation which can cover an extended volume in space. This sort of effect can completely envelop an ionization chamber such as used in this work giving a deflection of the electroscope equivalent to the dissipation within the sensitive volume of the system of several hundred mev in a fraction of a second. Since the effects of cosmic ray bursts are very distinctive, it is possible to study the discharge record of the electroscope, distinguish bursts larger than some minimum size and in part subtract out their effect on the discharge of the system. This point will be discussed in greater detail later.

The other effect from cosmic rays is due to their great penetrating power in conjunction with the general level of gamma radiation and high energy electrons which are a consequence of the mesons's passage through matter. With the equipment described here, this type of background radiation cannot immediately be distinguished from external gamma radiation. The only way this type of background radiation can be reduced is by shielding the equipment with "great quantities" of matter. "Great quantities" in this case means 200 meters-water-equivalent to reduce the level to less than 1% of the normal intensity.

In most measurements of radiation intensity, the measurement actually consists of two measurements, one of the background intensity and one of the background intensity plus the sample intensity, the result of interest being the difference of the two. In such a case, the statistics of the background radiation become just as important as that of the unknown sample to be measured, particularly if the background intensity and the sample intensity are of the same order of magnitude. As described above, background radiation and its effects on an ionization chamber are rather complex, and consequently, the statistics of the situation are also complex. However, there are certain general considerations which aid in the analysis of this situation; they may be stated as follows: If a single occurrence produces a large effect such as a cosmic ray burst or alpha particle might produce, the statistics must by necessity be poor. Assuming the occurrences are random, the number must be small if the total effect from such a source is not to be overwhelming. Conversely

if an effect is small, the statistics must be good in order that the total effect shall be of such a magnitude as to affect the situation significantly. The manner with which such considerations enter into the work described here will be discussed shortly.

Equipment Operation:

At this point, we have already described the basic measurement problem, some important considerations related to this problem, and the general design of the equipment intended to perform the measurement. We will now attempt to describe the detailed relationship of the equipment and its use in the solution of the problem.

The first requirement in making the measurement is putting the sample in a form suitable for measurement in this equipment. Since the measurement is on carbon-14 diluted by normal carbon to a very low specific activity, the equipment was designed to hold a large gaseous sample of carbon dioxide. Consequently, the carbon of the sample must be converted to carbon dioxide. In all instances involved in this work, the sample has been of an easily combustible nature; the samples were, therefore, burned converting any carbon directly to carbon dioxide. The combustion and purification equipment is pictured in photographs 19 and 20 and illustrated in drawings 9 through 12; the Appendix gives the details of the operation. The product of this purification is carbon dioxide which is both chemically and radiochemically purified to such an extent that the gas will perform satisfactorily as a chamber filling gas and the carbon-14 content can be measured without

interference from radioactive contamination within the gas. The carbon dioxide sample is next placed in the ionization chamber under a pressure adjusted to correspond to 125 psia at 27° C.

In order to reduce local internal contamination, the ionization chamber is constructed with certain special features. The first concerns the construction materials; previous workers (16, 17) have found that freshly machined steel is one of the better materials with respect to radioactive contamination. The system was therefore constructed of steel and the inside was freshly refaced just prior to assembly.

It has also been found that a layer of a radiochemically pure substance can aid in absorbing the alpha particles which may come from surface and volume contamination of the equipment construction materials. One approach to creating such a layer is to use a grid-walled system. In such a system, a grid is constructed and spaced a distance greater than the maximum alpha particle range from the wall of the chamber. The grid is designed to present as little surface area to the sensitive volume of the system as possible; with this equipment the grid wires are of 0.003" iron wire spaced 1/4" apart. This grid is maintained at a potential different than the chamber wall, such that any ionization produced between the wall and grid will not reach the sensing element of the system, the electroscope in this particular equipment. In this ionization chamber the electroscope operates at a potential of approximately 120 volts with respect to the chamber wall, and the grid operates at a potential of -30

volts with respect to the chamber wall. Since it is possible to measure physically the volume of the grid structure and of the complete chamber, it is possible to calculate the effect of the grid with regard to reducing the effective sensitive volume of the system. It is also possible to measure this effect directly. The indicated experiments were performed with the following results:

Calculated ratio of sensitive volume to total volume = 0.62 ± 0.02

Measured ratio of sensitive volume to total volume = 0.63 ± 0.03

The agreement is satisfactory.

Since a certain amount of contamination of the construction materials is due to surface absorption or adherence, another approach to contamination reduction is to treat the materials chemically so as to remove the surface layer. The removal of the surface layer was done mechanically in the case of the chamber wall; this mechanical method is not possible in the case of the grid structure; the chemical method was, therefore, used on the grid structure. This was accomplished, in practice, by a short soaking of the grid structure in conc. H_2SO_4 followed by rinsing in distilled water just prior to assembly within the equipment.

At this point the background radiation from sample contamination and internal contamination of the equipment has been presumably reduced. The system has also been designed to accept a large sample which will yield a large sample signal. The next problem is to consider the other sources of background radiation and the reduction of this radiation. The equipment is next placed under Morris Dam and in a lead house. The dam has a vertical material depth of 203 mwe which reduces the cosmic ray intensity

to the order of 1% of the surface intensity. The lead house reduces local external gamma radiation to the order of 1% or less. Actual experimental data indicates that the dam reduces the background level by a factor of approximately 50 with respect to cosmic rays and that the lead reduces the level by a factor of approximately 150 with respect to external gamma radiation; the combination reduces the background level by a factor of 200 which is less than the product due to the fact that the two shields do not interact greatly. That is, the dam does not reduce the external gamma radiation background being a source of such contamination; and the lead house does not reduce the cosmic ray background being insufficiently great in mass. In fact, the high atomic number of the lead increases the number of cosmic ray burst which occur near the equipment.

Conclusions:

At this point, all forms of background radiations have been reduced in some manner or other. The problem now is to analyze the data obtained with this equipment and determine just how successful the reduction has been. Typical discharge traces obtained with this equipment appear in photographs 25, 26 and 27. The first obvious but unexplained feature of the traces is the occasional sudden displacements; two excellent examples appear on pictures 26 and 27. These sudden displacements are due to cosmic ray bursts. It is possible to measure the size of such obvious effects and to subtract out their effect on the discharge of the electroscope

and the trace in which they appear. It is also possible to consider only traces, such as pictured in photograph 25, which contain no obvious bursts whatsoever. However, one must consider the problem of bursts which are too small to be resolved by this recording system. This may be done in the following way: Considerable work has been done concerning the nature of the cosmic ray burst size spectrum. Of particular interest is the work of Schein and Gill (18). Their work was done with an ionization chamber system whose relative sensitivity may be compared with that of the equipment described here. Their data includes sufficient numbers to give results of reasonable statistical reliability. Graph 7 illustrates a comparison of their data and the limited data obtained during this work. If one now extrapolates this data to small burst sizes, one obtains the following results. For a burst size of 0.5 on the arbitrary scale one would expect perhaps a cumulative number of about 160, or 79 bursts of size 0.5 only. This data covers a period of about 240 hours. Since a discharge trace requires roughly 3 hours, this represents approximately 1 burst of this size per discharge trace. A burst of this size represents an actual displacement of 0.005 centimeters; a trace representing normal background radiations has an overall displacement of approximately 0.5 centimeters; therefore, bursts of this size represent 1% of the total background discharge on the average. Thus regardless of the background statistics, a fluctuation on the order of 1% would be expected from cosmic ray bursts of this size. For bursts of smaller size the magnitude of the net effect is smaller both because of the smaller size of the bursts and because of their increased number.

If one considers actual data obtained with this equipment one finds that the situation is perhaps somewhat better than the above analysis predicts. For example, the displacement of 5 background traces was measured carefully with a traveling microscope. This was done for each time marker on the film, and any obvious cosmic ray bursts were measured and subtracted from the data. From this data, the rate of discharge for each trace was calculated by way of two approaches to the interpretation of the data. In the first approach, each time period is considered as a separate independent measurement. The displacement between each time marker and the next was measured, and the various values for each trace were averaged. The results obtained are as follows:

Film	Displacement Increment Average
19 July '55	0.00552 cm/min.
21 July '55	0.00555
25 July '55	0.00558
29 July '55	0.00544
31 July '55	0.00562
Average	0.00554 cm/min.
Probable error	0.74%
Spread	3.2%

The individual values of the displacement increment averages represents the average of approximately 35 separate measurements per film. If one calculates the statistical error in these values based on the apparent random variations of the 35 distinct measurements, one finds that this value has a probable error of

approximately 5%. Note however, that the agreement between the five different films is far better than this.

In the second approach, the best slope or displacement rate was determined by the method of least squares using the same data as used above. The results are as follows:

Film	Slope or Displacement Rate
19 July '55	0.00546 cm/min.
21 July '55	0.00541
25 July '55	0.00559
29 July '55	0.00543
31 July '55	0.00553
Average	0.00550 cm/min.
Probable error	0.69%
Spread	2.9%

If one calculates the statistical error in the values of the displacement rate for each film based on a least squares analysis of the various 35 or more separate measurements per film trace, one finds that this value of displacement rate has a probable error of approximately 0.4%. Note however, that the agreement between the 5 different films is far worse than this. If one considers the difference between the values for each film determined by the two approaches, one finds that on the average the values differ by approximately 0.8% which is approximately equal to the probable error in the 5 film average as determined by either method and also the difference between the two averages. The agreement between the two methods for each film indicates that the slope of each trace is well defined. However, the larger fluctuation from film to film indicates some definite variation from one film to the

other; this is due presumably to cosmic ray bursts of small size. It should be noted that the effects observed are of the correct order of magnitude as determined by the previous analysis.

Perhaps the next most apparent feature of the discharge trace is the uniform slope exclusive of the cosmic ray bursts. This is, of course, as desired. The data cited above indicates the uniformity of the discharge rate. At this point, the results of several experiments intended to determine certain characteristics of the system can be discussed assuming that we now have a satisfactory radiation measuring system. As indicated previously, the material shielding of the concrete in the dam and the lead house reduced the background considerably. It was found that the measured background within the lead shield but outside of the dam gave an electroscope discharge rate approximately 50 times that which was observed under the dam. It was also found that under the dam but outside of the lead shield the discharge rate was approximately 100-150 times as fast as within the lead shield. The combined shielding of the dam and the lead house yielded a discharge rate roughly 1/200th of that observed without any shielding. It should be noted that when the equipment is not under the dam the background discharge rate is both rapid and very irregular; therefore, the values quoted are only roughly correct.

In previous considerations, an estimate was made concerning the level of the carbon-14 radiation contained in a carbon dioxide sample in exchange equilibrium with the carbon reservoir.

The ratio indicated was 10 to 0.2 ion pairs per cubic centimeter per second or 50 to 1. With the aid of the above measured ratios and the measured discharge rate due to a modern carbon sample, this estimate may be checked. It was found that normal background radiation under Morris Dam and within the lead house gave an average discharge rate of 4.25×10^{-3} cm/min. and a modern carbon sample plus background radiation gave a discharge rate of 8.22×10^{-3} cm/min. The difference, or 3.97×10^{-3} cm/min., represents a ratio of 0.93. Considering the previously determined ratio of 1/200 multiplied by 0.93, one concludes that the radiation intensity due to the carbon-14 in a modern sample is roughly 1/200th of normal background radiation intensity. This ratio is somewhat smaller than the predicted one; however, considering the problems of such an estimate, the agreement is satisfactory.

We now come to the very important problem of attempting to determine the nature or cause of the background radiation observed with this equipment. That is, after all the measures have been taken to reduce background radiation, what now is the cause of the remaining observed background radiation? One of the first experiments performed in this connection concerned the function of the grid structure. If there is a significant amount of alpha particle emitting contamination on or in the chamber walls, it should be possible to reduce the pressure of the filling gas to such a point that these alpha particles will penetrate the grid structure and thus enter the sensitive volume of the system

contributing to the observed background radiation. Graph 5 illustrates the results of these experiments, and as predicted, at lower pressures the background radiation intensity increases. The magnitude of the increase indicates that this source of background would be quite important if not for the grid structure. It should be noted at this point, however, that with any source of naturally occurring alpha radiation, there is always associated beta and gamma radiation. If one considers the natural radioactive series, he will find that the number of alpha and beta disintegrations are roughly equal, and taking into account the density of the sensitive volume in this system, the beta rays will contribute a not insignificant amount to the background radiation as compared to that from alpha radiation. Consequently, although the background due to alpha radiation may be reduced by the grid structure, the associated beta and gamma radiation must remain and be of some significance.

Returning now to external material shielding, it is difficult to decide whether a significant amount of background is due to their inadequacy. In order to clarify this situation, the equipment was moved to a deeper location. If a major portion of the background radiation is due to cosmic rays, this change should cause an observable effect. If not, little effect should be observed assuming, of course, that the local external contamination remains constant. If, however, the local external contamination is changed, an effect due to this type of background should be observed. To perform this experiment the equipment was moved

to a limestone mine near Riverside, California. This location is at a depth of 267 meters-water-equivalent as compared to 203 meters-water-equivalent at the Morris Dam location. By considering data obtained by V. C. Wilson (19), one would expect cosmic rays to be 0.40% of the surface of intensity at 267 mwe and 0.70% at 203 mwe, a ratio of 1 to 1.75. The observed effect represents a ratio of 1 to 1.65 which is in close agreement with the estimate. This would indicate that the major portion of the background radiation is due to cosmic rays. However, the conclusions are not entirely clear cut due to the fact that the local external contamination is expected to be lower at this new location also. Nevertheless, the results indicate one important, clear cut fact; the background radiation is to a great extent due to external sources of ionizing radiation and not due to internal contamination of the equipment. It should be noted that the increase in discharge rate due to a modern carbon sample over that due to background radiation for the two locations agrees within experimental error, being 3.97 ± 0.17(S.D. $\times 10^{-3}$ cm/min. at the Morris Dam location and 3.87 ± 0.16(S.D.) $\times 10^{-3}$ cm/min. at the Riverside location. It should also be noted that at this new location the ratio of the discharge rate due to a modern carbon sample and that due to background has increased from 0.93 to 1.47. Since the major cause of variation in discharge rate is apparently due to cosmic ray bursts and the major cause of the background radiation is apparently the cosmic rays themselves,

it would seem possible to improve the situation greatly by using an equipment location which is deeper underground. Although with this type of equipment this sort of approach to the reduction of background radiation and its effects is very effective, this approach should be worthwhile with all types of equipment to some extent. Although such equipment locations, as suggested here, are rather inconvenient, it is surprising that such locations have not been made use of to a greater extent.

APPENDIX

Photograph No. 3 This is the entrance to the side road which leads to the base of Morris Dam.

Photograph No. 4 It was necessary to ford the above stream in order to reach the base of the dam. The stream flows at the bottom of the canyon below the dam.

Photograph No. 5 This picture is a backward view showing the course of the road down the canyon wall.

Photograph No. 6 This is a view from the base of the dam down the canyon. Note the small lake in the foreground.

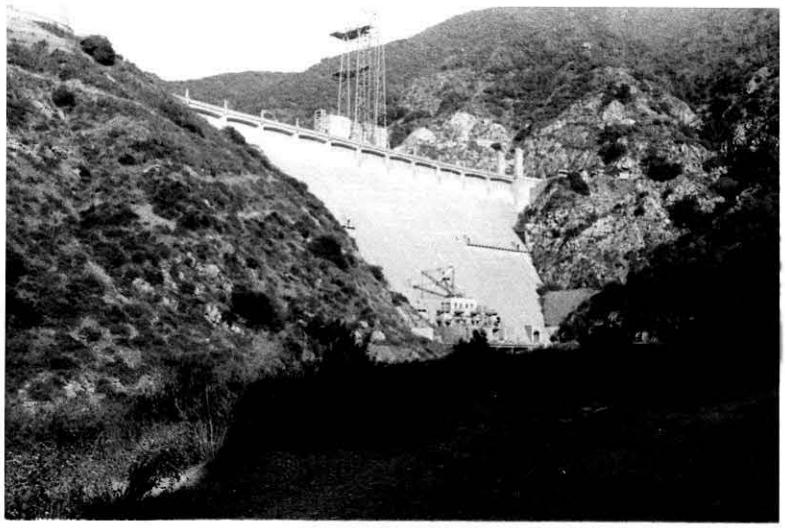

Photograph No. 7 Morris Dam. The first full view of the dam as seen from the side road is shown here.

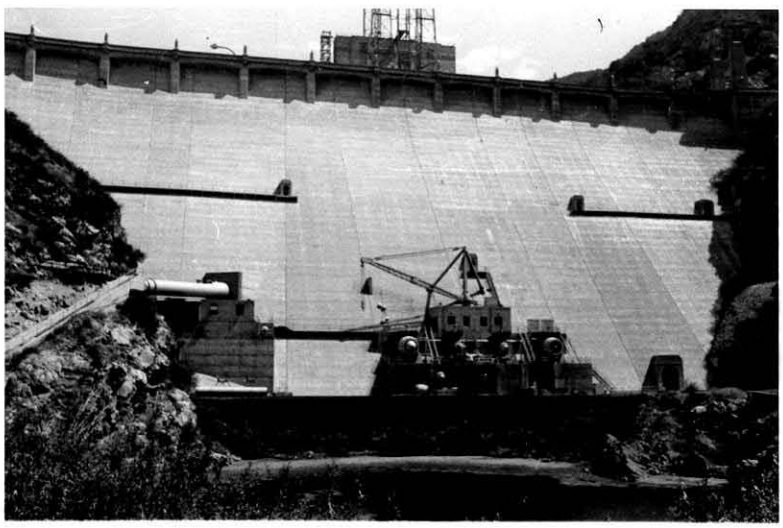

Photograph No. 8 A closer view of the dam is shown here.

Photograph No. 9 This is a view of the bottom of the dam. The entrance to the 937 ft. gallery is through the second opening from the right, the one from which the wooden trough protrudes.

Photograph No. 10 The entrance and gate to the 937 ft. gallery is pictured here. Note that shortly after the previous picture was taken and prior to the taking of this one, the wooden trough collapsed and is now seen approximately in the center of the photograph.

Photograph No. 11 The tunnel seen in photograph 10 leads straight under the dam for approximately 175 ft. at which point it is perhaps 20 ft. from the water. Here it intersects a perpendicular tunnel. In this picture you see the left half of this tunnel. This is the tunnel where the equipment was set up.

Photograph No. 12 This is a view of the equipment in the tunnel pictured in photograph 11. Note in the foreground the intersection of this tunnel with the main tunnel of photograph 10.

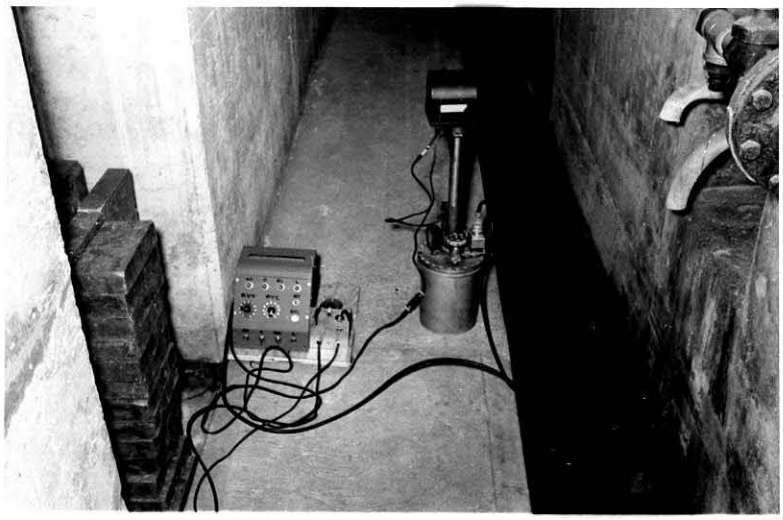

Photograph No. 13. The equipment is shown here set up and ready to be put into operation short of placing the ionization chamber, which is seen on the right, within the lead shield, which is seen on the extreme left.

Photograph No. 14 This is a close view of the timing and control equipment. On the left is seen the box containing the recharging voltage batteries, the camera power supply, the light source power supply and the recharging cycle timing and activation device. On the right is seen the time marking device.

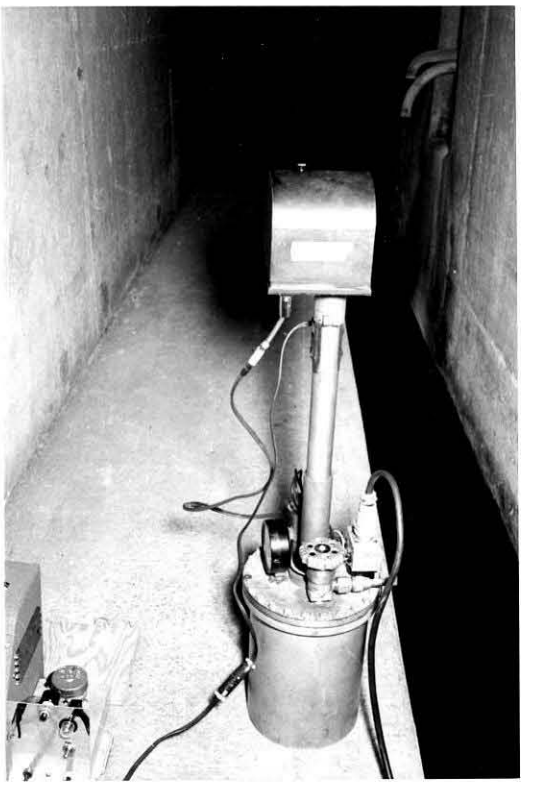

Photograph No. 15 This is a close view of the ionization chamber and associated equipment. Note the following: the camera at the top on the end of the optical tube, the ionization chamber supporting the optical tube and on the chamber (front) the high pressure valve, (right) the power cable connection and junction box, (rear, just behind the optical tube) the light source, and (at the left) the chamber pressure gage. Note also the power cables leading to the camera and the time marking light mounted on and near the top of the optical tube.

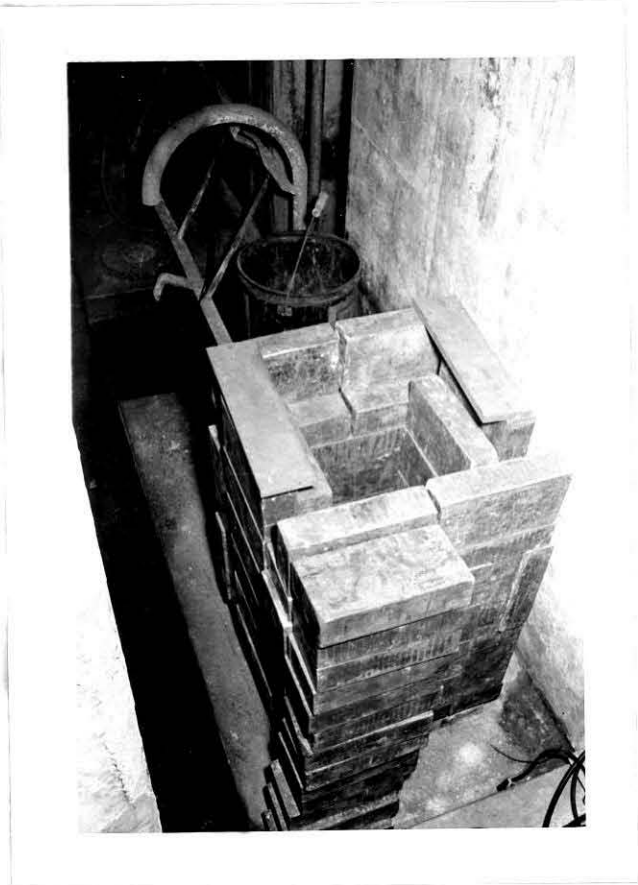

Photograph No. 16 A close view of the empty lead house is shown here. Note that the lead bricks for the lid are piled just in front of the lead house.

Photograph No. 17 This picture shows the ionization chamber and attached equipment in the lead house with the lid in place. The equipment as seen here is in the operating arrangement. Note the control box in the foreground.

Photograph No. 18 This view is of the entire setup including cover cloths which partially protect the equipment from moisture and falling dirt.

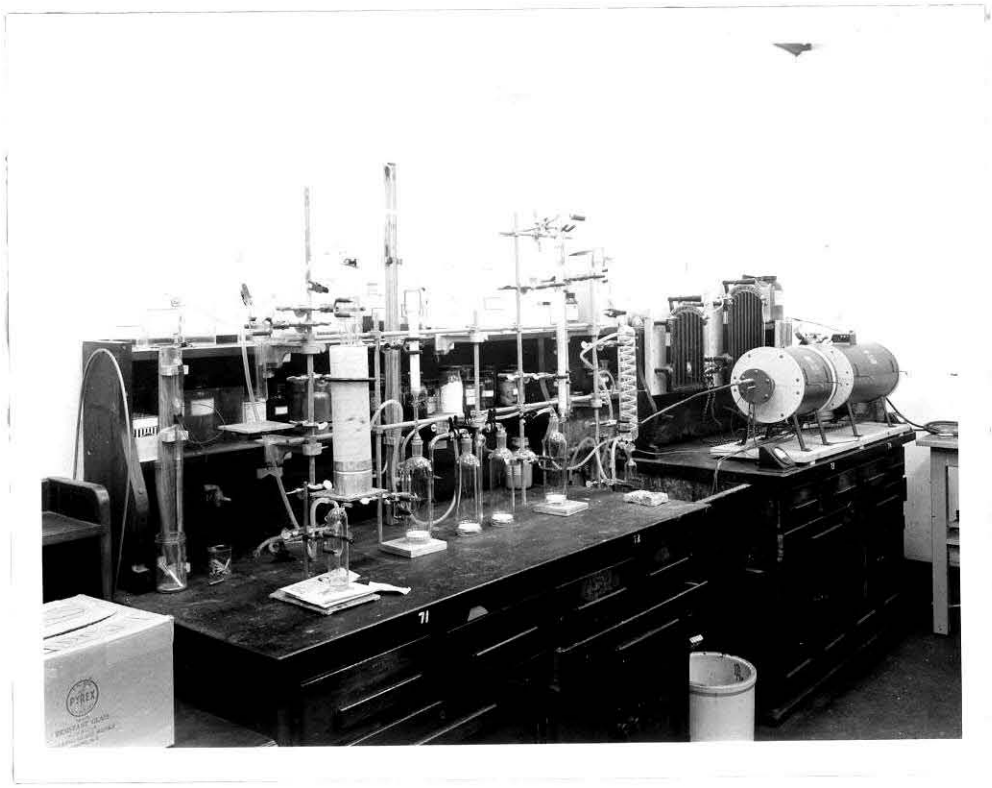

Photograph No. 19 This picture was taken in room 21 of the Gates Laboratories of Chemistry at the California Institute of Technology. It shows the sample combustion furnaces (in the background) and the carbon dioxide purification line (in the foreground).

Photograph No. 20 Again in room 21, this picture shows the high-vacuum system (in the background) and associated equipment. Note the diffusion pump on the left, the liquid nitrogen Dewar in foreground and the sample cylinder on the right.

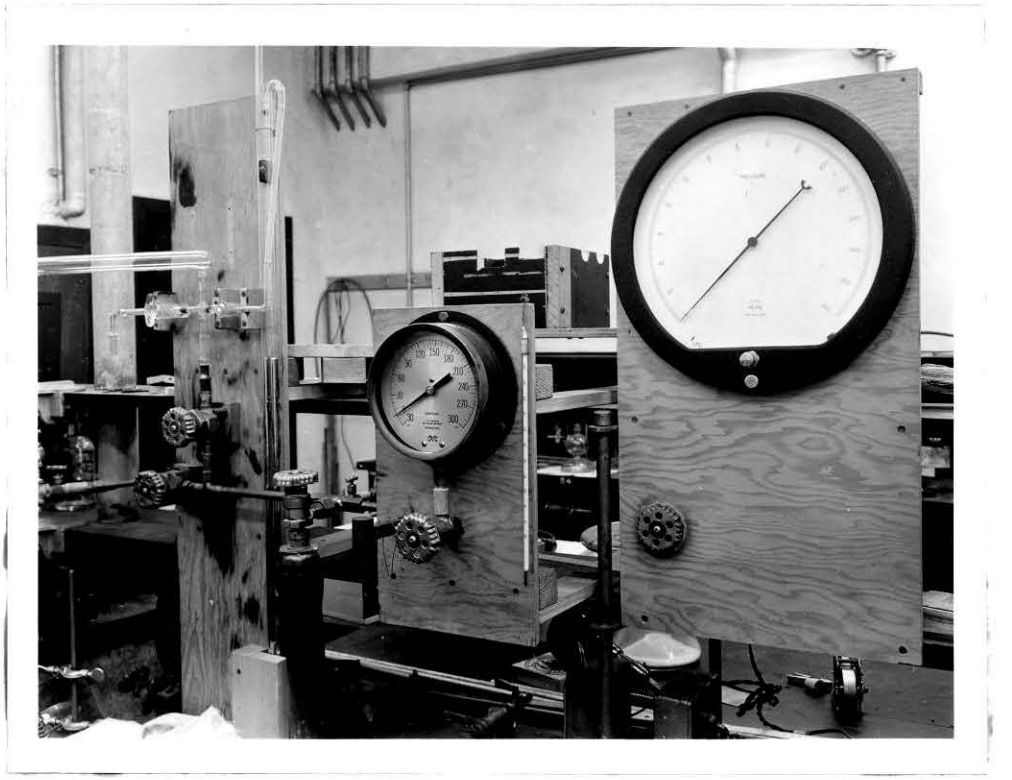

Photograph No. 21 Also in room 21, this picture is of the high pressure chamber filling system. This equipment was modified slightly after this picture was taken; however, it is included since it gives a clear view of the high pressure Heise gage used for high pressure measurements.

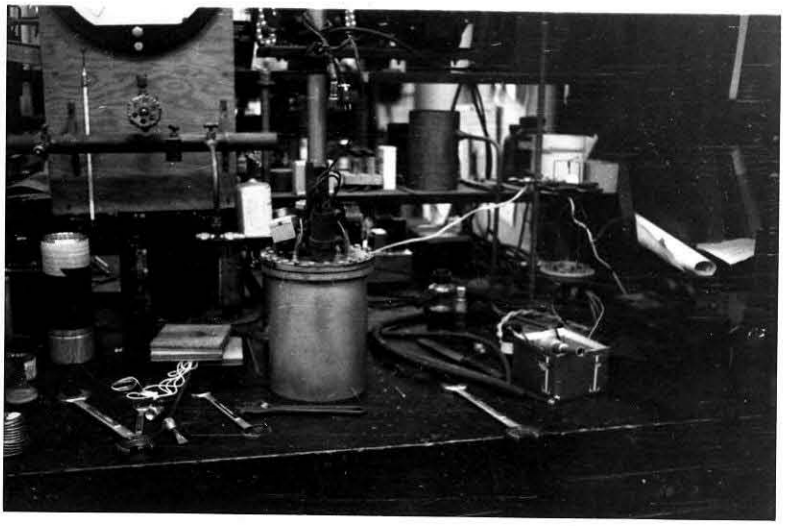

Photograph No. 22 This picture illustrates the final high pressure manifold with the ionization chamber connected to the system. The bottom of the Heise gage may be seen at the top of the picture.

Photograph No. 23 This is a picture of a typical sample storage cylinder. This cylinder is a war surplus oxygen cylinder with the addition of a high pressure valve.

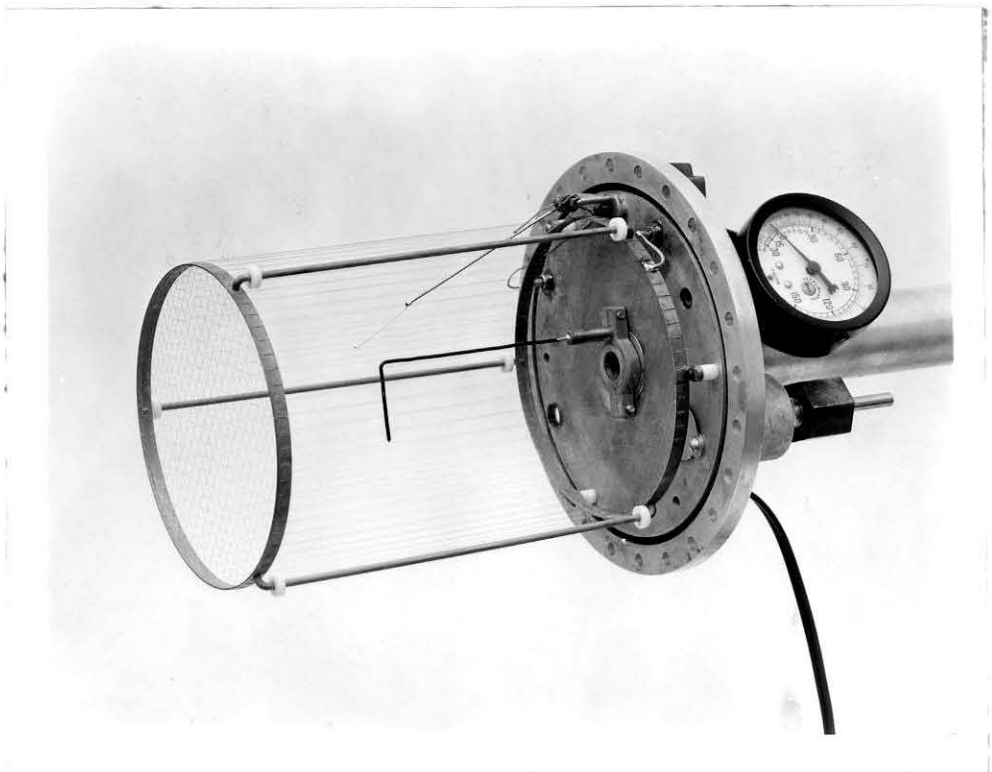

Photograph No. 24 This picture is of a preliminary mock-up of the ionization chamber system. The final electroscope mounting and optical system were changed in the final equipment. However, the details of the recharging arm and the grid structure appear essentially as in the final equipment.

Photograph No. 25 The camera is illustrated in this picture. The camera lid and securing screw are seen on the left. Note the film on the film drum as it normally appears and the synchronous drive motor. This motor has a speed of 1 rpm and by means of a worm gear train, which is not seen in this picture, the drum is driven at a speed of approximately 1/50 R. P. H.

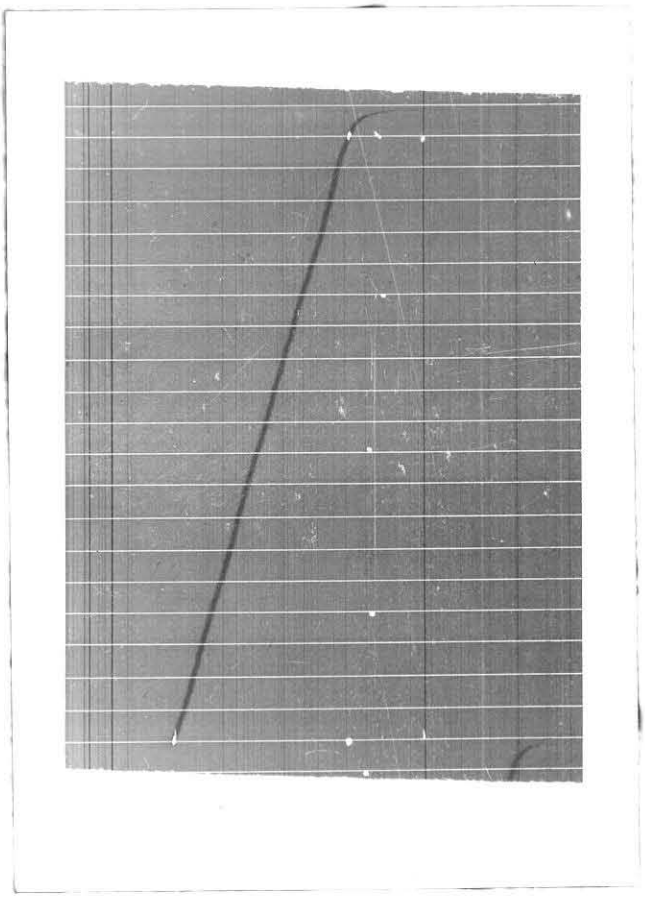

Photograph No. 26. This is a positive print of an actual discharge trace. The sample contained in the system was of lead carbon dioxide, and therefore, this represents a typical background discharge trace. Note the horizontal lines which are the time marking lines. It is perhaps possible to observe here the variations in distance between these lines which are due to the irregular speed of the film drum. Note also the vertical background lines which are due to dirt on the optical slit. These lines are very useful since they show the precise direction of travel of the film.

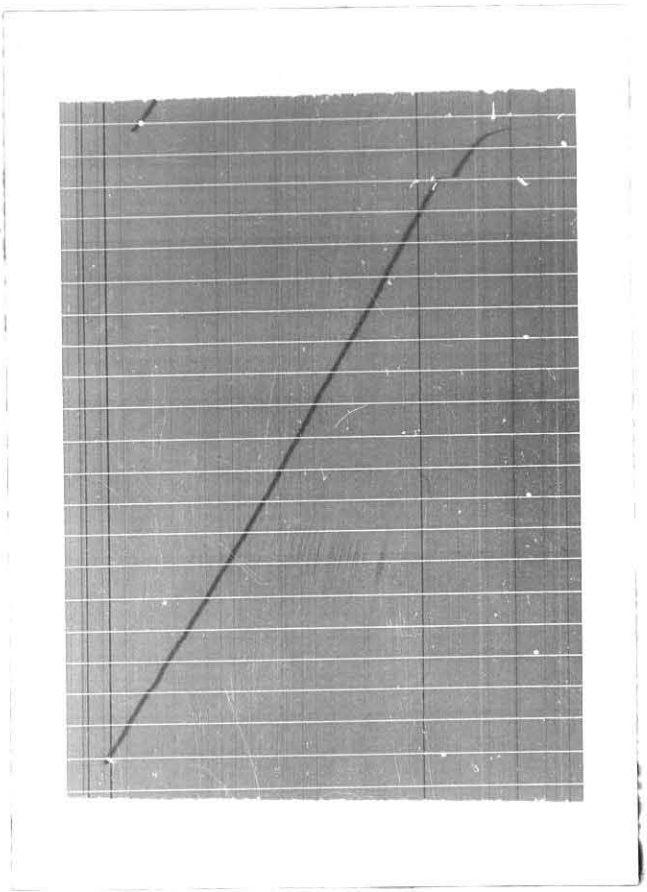

Photograph No. 27 This again is a positive print of a discharge trace; in this case the sample is of modern carbon. This trace was shown here since it includes at least three cosmic ray bursts. The most obvious is near the top and is quite large. Two more appear near the fourth and sixth time marking lines counted from the bottom of the picture.

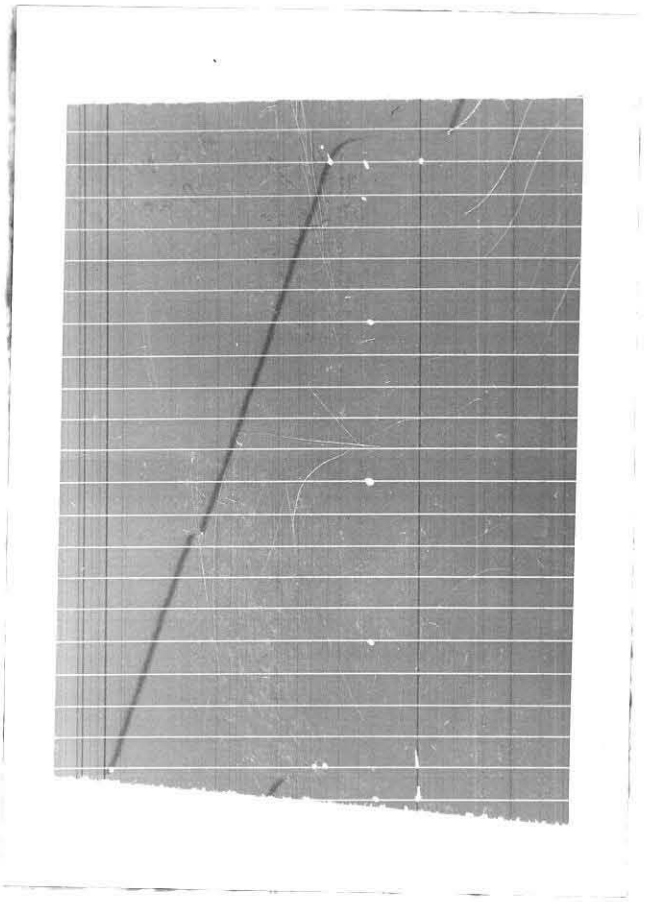

Photograph No. 28 This is a trace from a sample from the La Brea tar pits and is calculated to be approximately 16,700 years old. This trace also includes a relatively large cosmic ray burst.

GRAPH 1

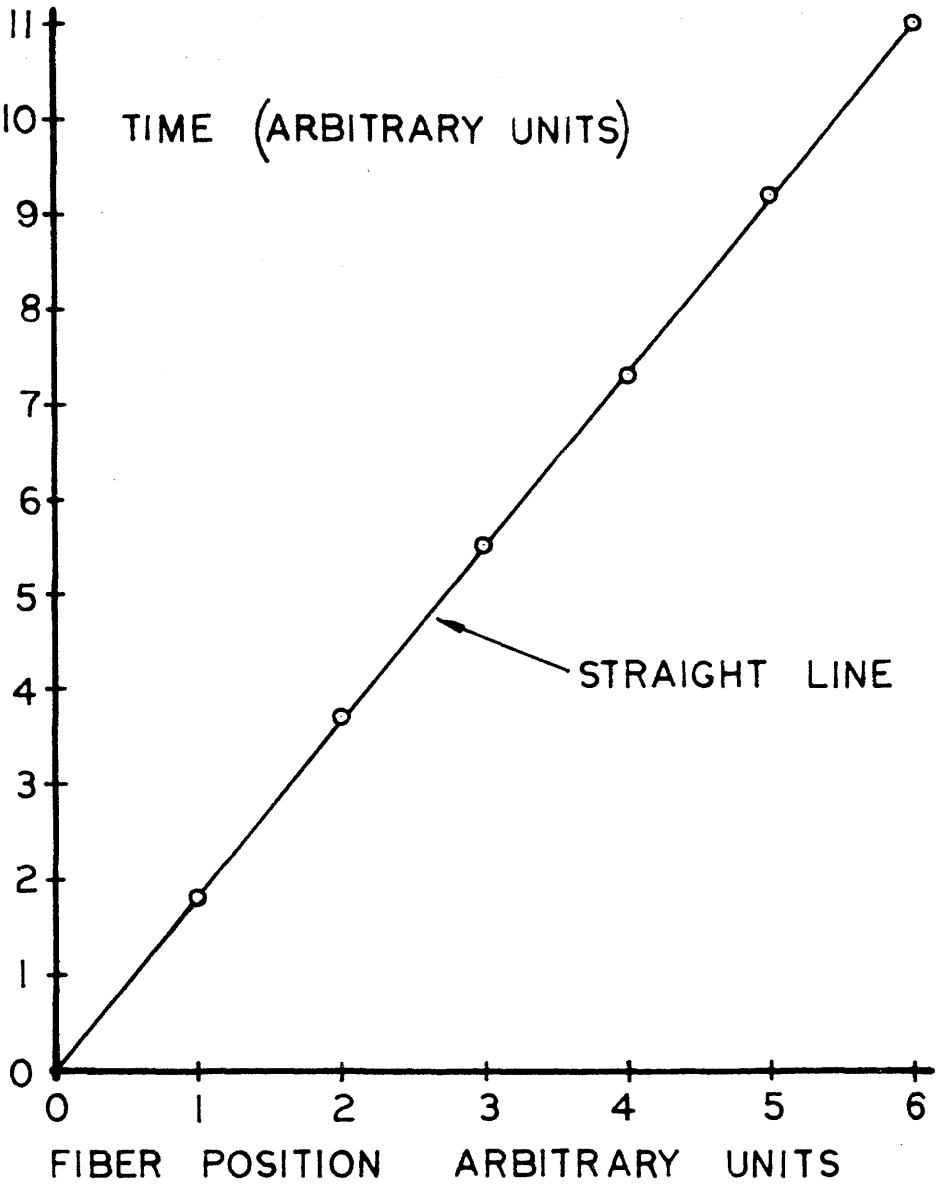

ELECTROSCOPE LINEARITY.

(DATA, THE AVERAGE OF THREE RUNS MADE UNDER MORRIS DAM OUTSIDE OF LEAD SHIELD)

NFJ

GRAPH 2

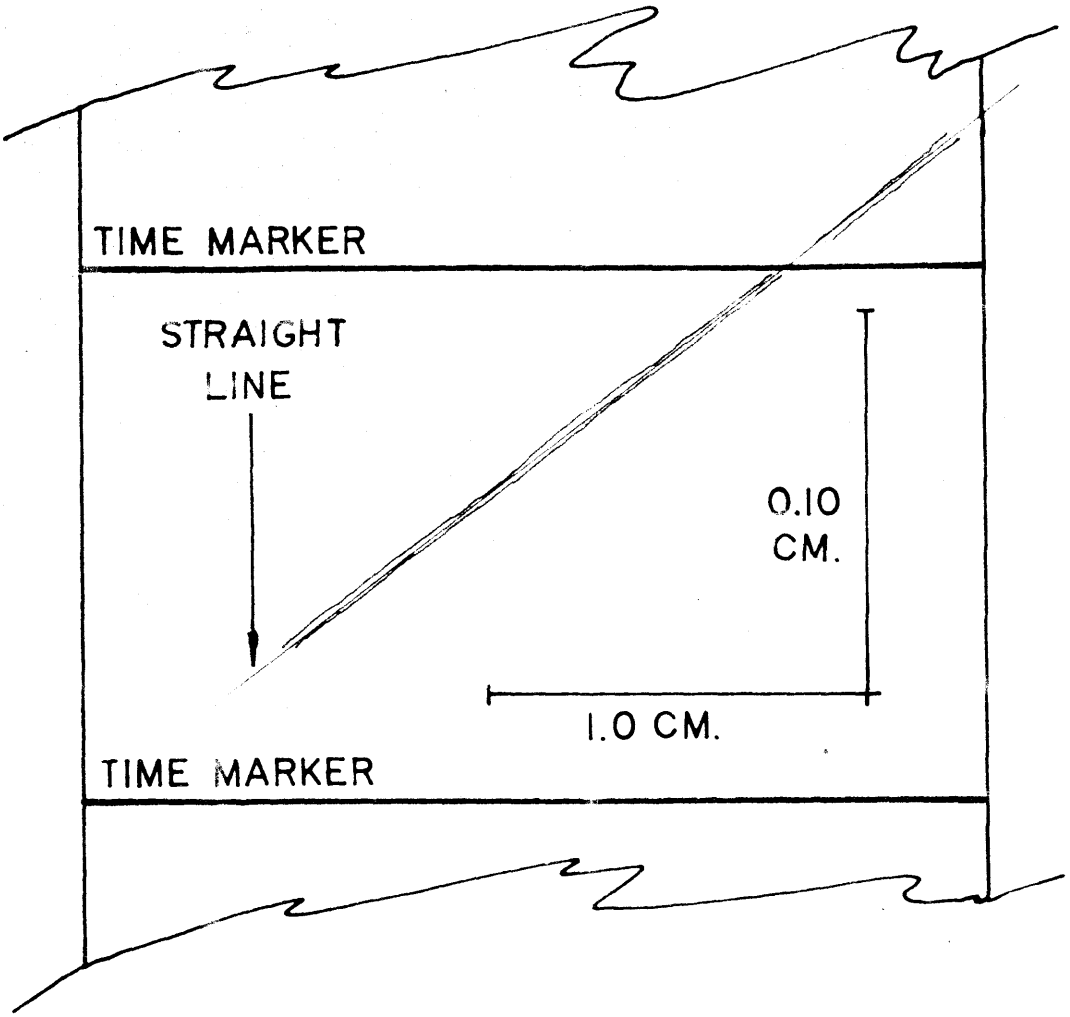

ELECTROSCOPE LINEARITY.

ACTUAL OUTLINE OF A DISCHARGE TRACE AS VIEWED ON ANISOTROPIC ENLARGER.

NOTE: TIME MARKER LINES AND ENLARGEMENT DIMENSIONS.

NFJ

GRAPH. 3

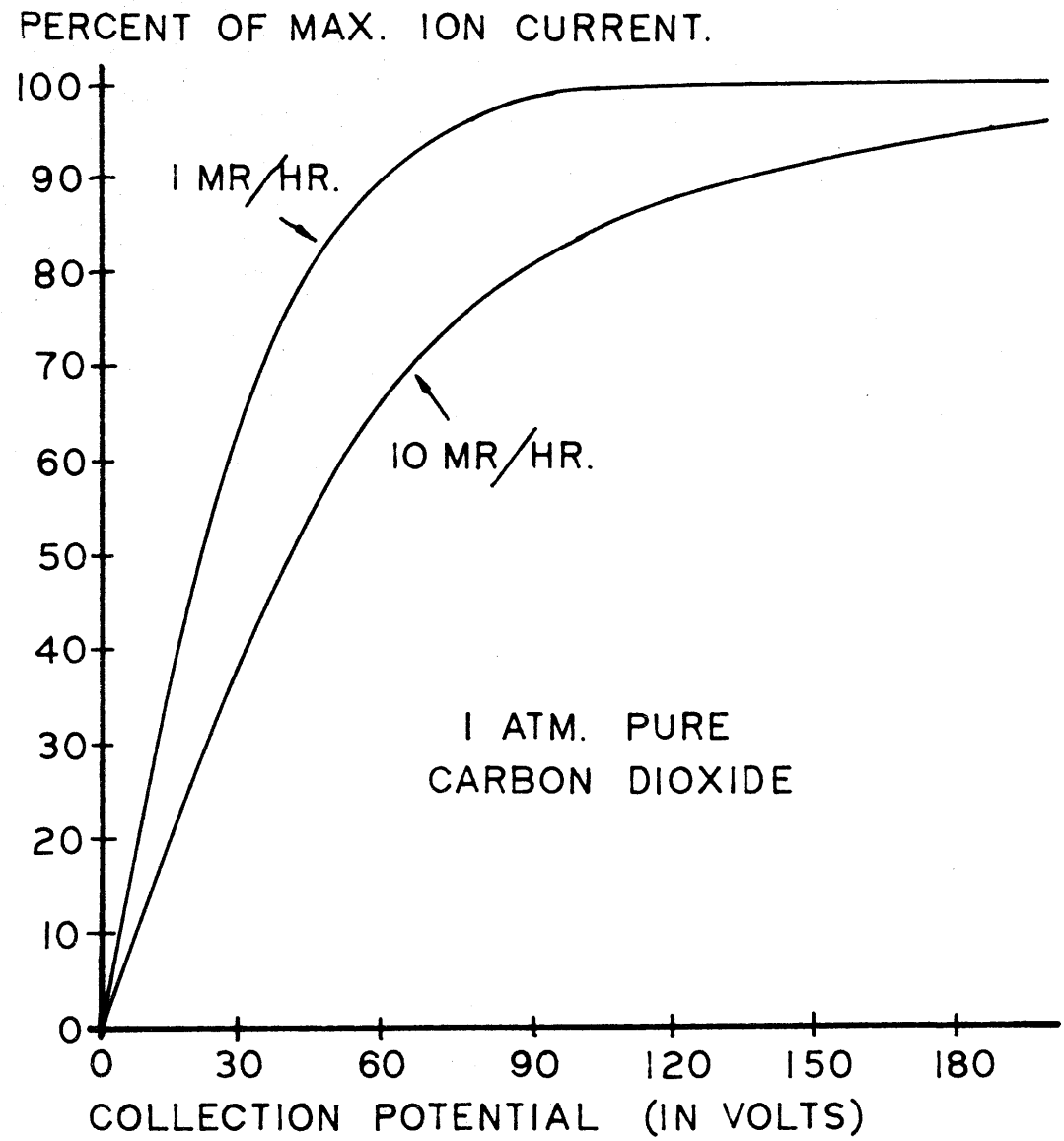

IONIZATION CHAMBER CURRENT SATURATION CURVES.

NFJ

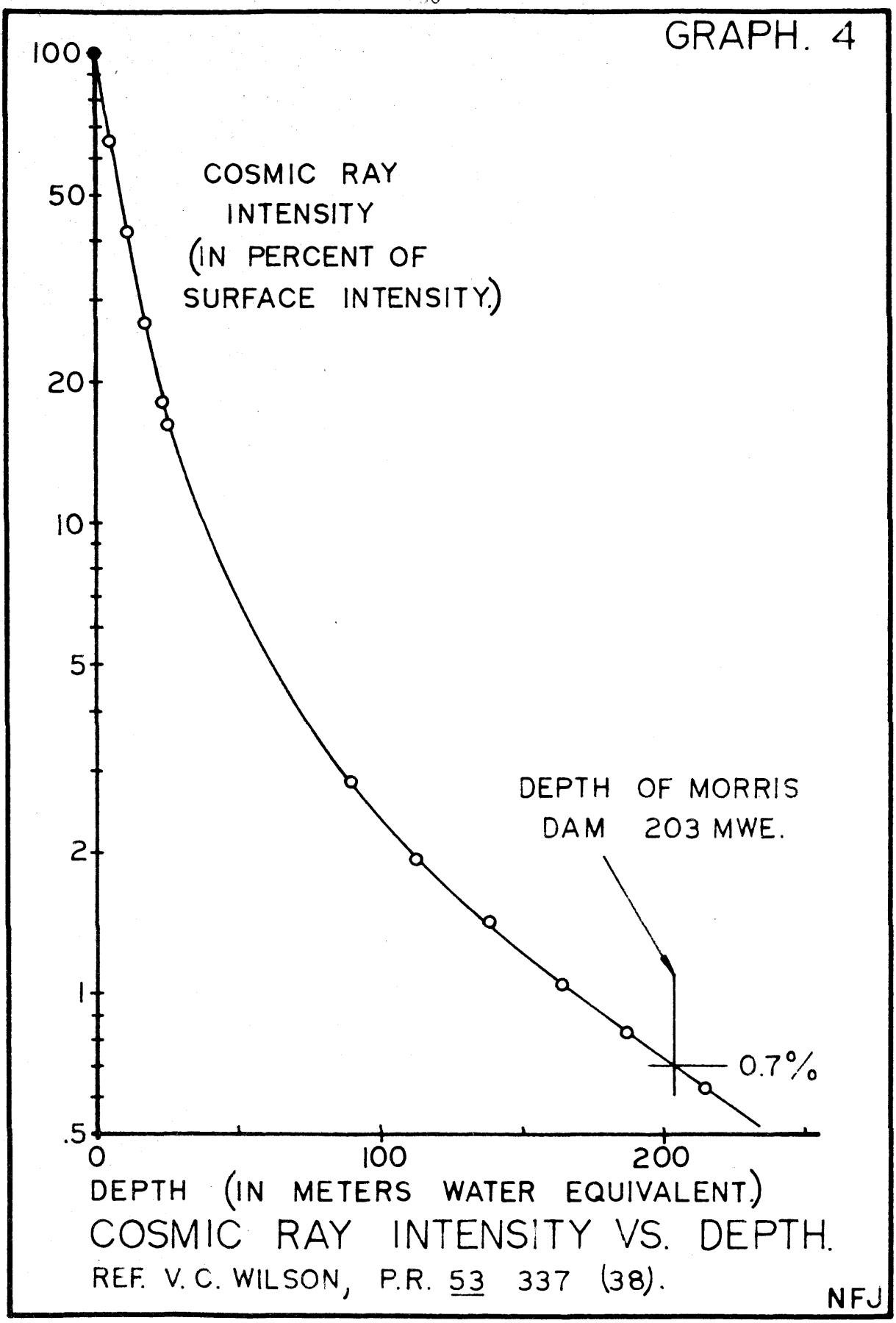
GRAPH. 4
100
50
20
10
5
2
1
.5
COSMIC RAY
INTENSITY
(IN PERCENT OF
SURFACE INTENSITY.)
DEPTH OF MORRIS
DAM 203 MWE.
0.7%
0
100
200
DEPTH (IN METERS WATER EQUIVALENT.)
COSMIC RAY INTENSITY VS. DEPTH.
REF. V. C. WILSON, P.R. 53 337 (38).
NFJ

GRAPH. 5

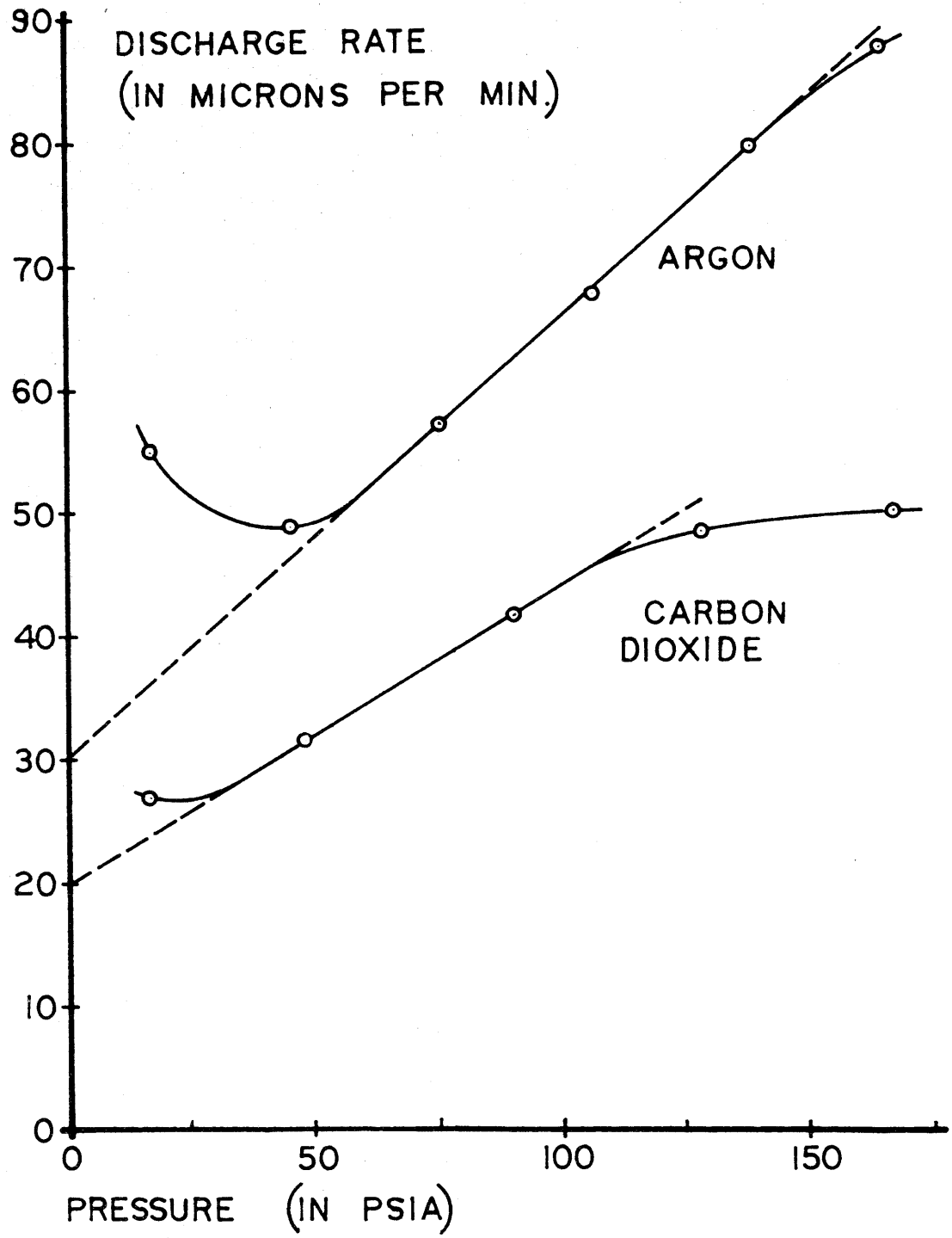

DISCHARGE RATE VS. PRESSURE FOR NORMAL BACKGROUND.

NFJ

GRAPH. 6

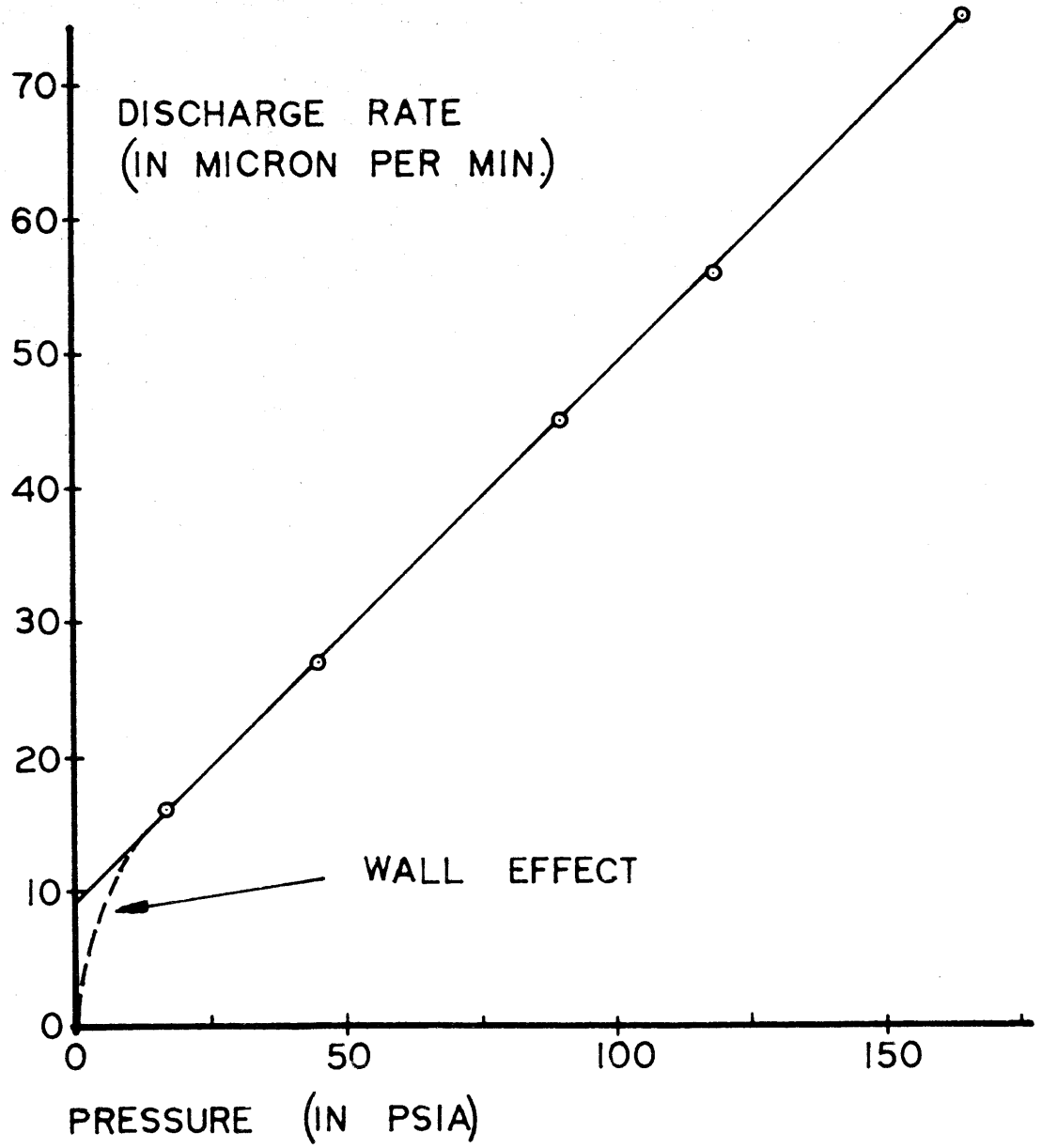

DISCHARGE RATE VS. PRESSURE FOR COBALT – 60.

(APPROX. 2 MC. WAS PLACED 100 CM. FROM THE LEAD SHIELD UNDER MORRIS DAM. ALL VALUES EXCLUSIVE OF BACKGROUND.)

NFJ

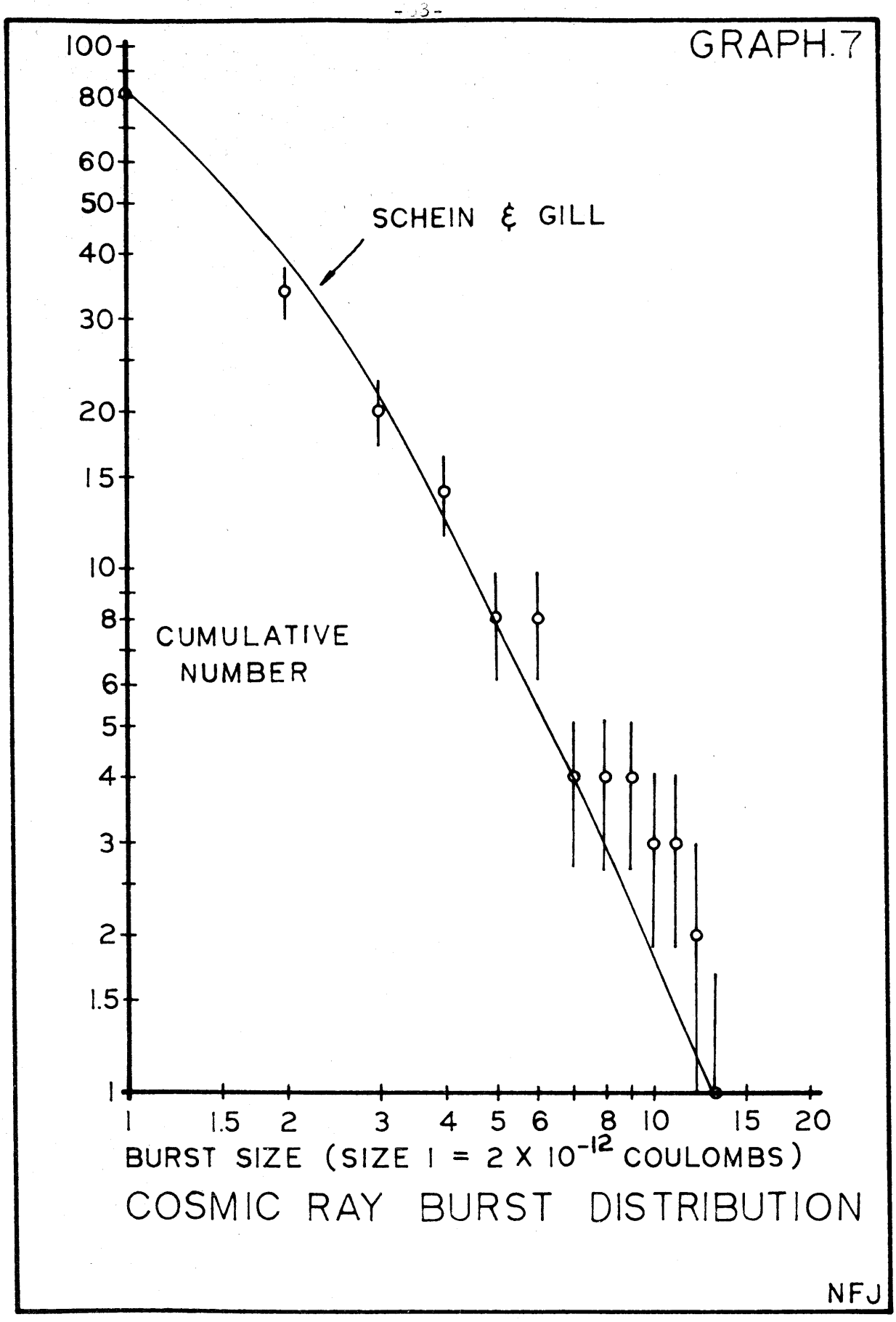
GRAPH.7
100
80
60
50
40
30
20
15
10
8
6
5
4
3
2
1.5
1
SCHEIN & GILL
CUMULATIVE
NUMBER
1
1.5
2
3
4
5
6
8
10
15
20
BURST SIZE (SIZE 1 = 2 X 10^-12 COULOMBS)
COSMIC RAY BURST DISTRIBUTION
NFJ

GRAPH. 8

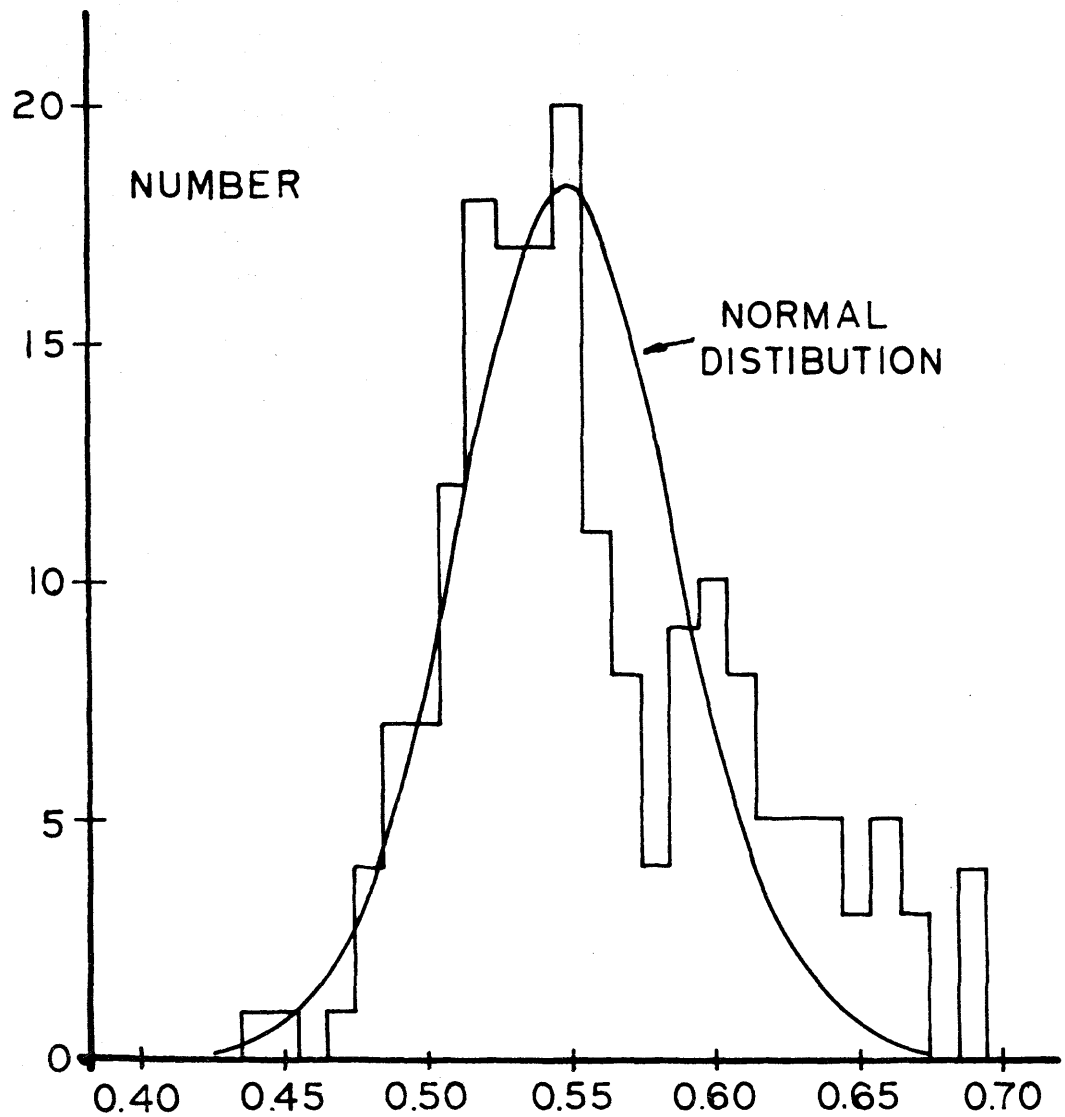

HISTOGRAM OF DISPLACEMENT INCREMENTS (FOR 5 BKGD. TRACES)

NFJ

Graphs:

Graph 1. Electroscope Linearity.

The data represented in this graph was obtained under Morris Dam with the equipment outside of the lead shield. The experiment was performed under these circumstances in order to obtain a low radiation intensity which was uniform in time. The experiment was originally performed in the laboratory under the lead shield; it was found that under such circumstances the large number of cosmic ray bursts produced in the lead shield yielded a radiation field with large and numerous variations.

Graph 2. Electroscope Linearity

This is the actual outline of a rapid discharge trace which was produced under Morris Dam. The equipment was in the lead house and a 3 millicurie Cobalt-60 source was brought within a few feet of the lead house yielding a relatively strong uniform radiation field. Note that the picture has been enlarged anisotropically and that the distance between time markers is exactly ten minutes.

Graph 3. Ionization Chamber Current Saturation Curves

This graph is the result of some experiments on a mock-up of the electroscope and ionization chamber system. The radiation intensity was measured with a monitoring instrument and the collected ion current with a high meg resistor and electrometer tube system. Normal background is approximately 0.02 milliroentgen per hour in the laboratory and estimated

to be 0.001 milliroentgen per hour under Morris Dam within the lead house. This data was intended to indicate the quality of the carbon dioxide as a filling gas for the ionization chamber.

Graph 4. Cosmic Ray Intensity versus Depth

This drawing is a reproduction of some data by V. C. Wilson (P. R. 53, 337, 1938) on cosmic ray intensity versus depth underground. The vertical depth of the Morris Dam location and the cosmic ray intensity estimated from this data are indicated on the drawing.

Graph 5. Discharge Rate versus Pressure for Normal Background

This graph illustrates the results of experiments on the variation of discharge rate due to background radiation with change in filling gas type and filling gas pressure. The observed increase in discharge rate at low pressures is believed to be due to the penetration by alpha particles into the sensitive volume of the system. At higher pressures these alpha particles which presumably originate in and on the chamber walls are stopped by the layer of filling gas lying between the wall and grid structure. The drop off in discharge rate at higher pressures is believed to be due to the effects of recombination and/or unsaturation of the ionization chamber. The extrapolations of the linear portions of these curves do not pass through the origin; this is believed to be due to pressure independent sources of ionization such as alpha contamination and the transition from a volume ionization chamber type of operation to a cavity chamber type of operation.

Graph 6. Discharge Rate versus Pressure for Cobalt-60

This graph illustrates the discharge rate versus pressure for a definite known intensity of gamma radiation as produced by a 3 millicurie cobalt 60 source. This source was placed approximately 1 meter from the lead house under Morris Dam. The data represented here has had the discharge rate due to background radiation subtracted from it. It is noticed here as in graph 5 that the curve apparently does not pass through the origin; this is believed to be due to the same cause, a transition from a volume chamber operation to a cavity chamber operation. Since the curve must pass through the origin the dotted line labeled wall effect has been included. It should be noted that exclusive of this wall effect the relationship of pressure to discharge rate is linear as theory predicts.

Graph 7. Cosmic Ray Burst Distribution

This graph is a comparison of the data obtained by Schein and Gill (18) on cosmic ray burst size versus frequency and the limited data obtained during this work. From the agreement of the two data an estimate of the contribution to discharge rate of cosmic ray bursts too small to be resolved on this equipment can be made.

Graph 8. Histogram of Displacement Increment

This histogram is of data taken from five background discharge traces. The displacement between succeeding individual time markers has been plotted against number. All apparent cosmic ray bursts have been eliminated from this data. Superimposed on this histogram is a normal or Gaussian distribution

with the same mean and dispersion; it can be seen that the histogram is somewhat weighted on the side of the larger displacements.

FIG. 1

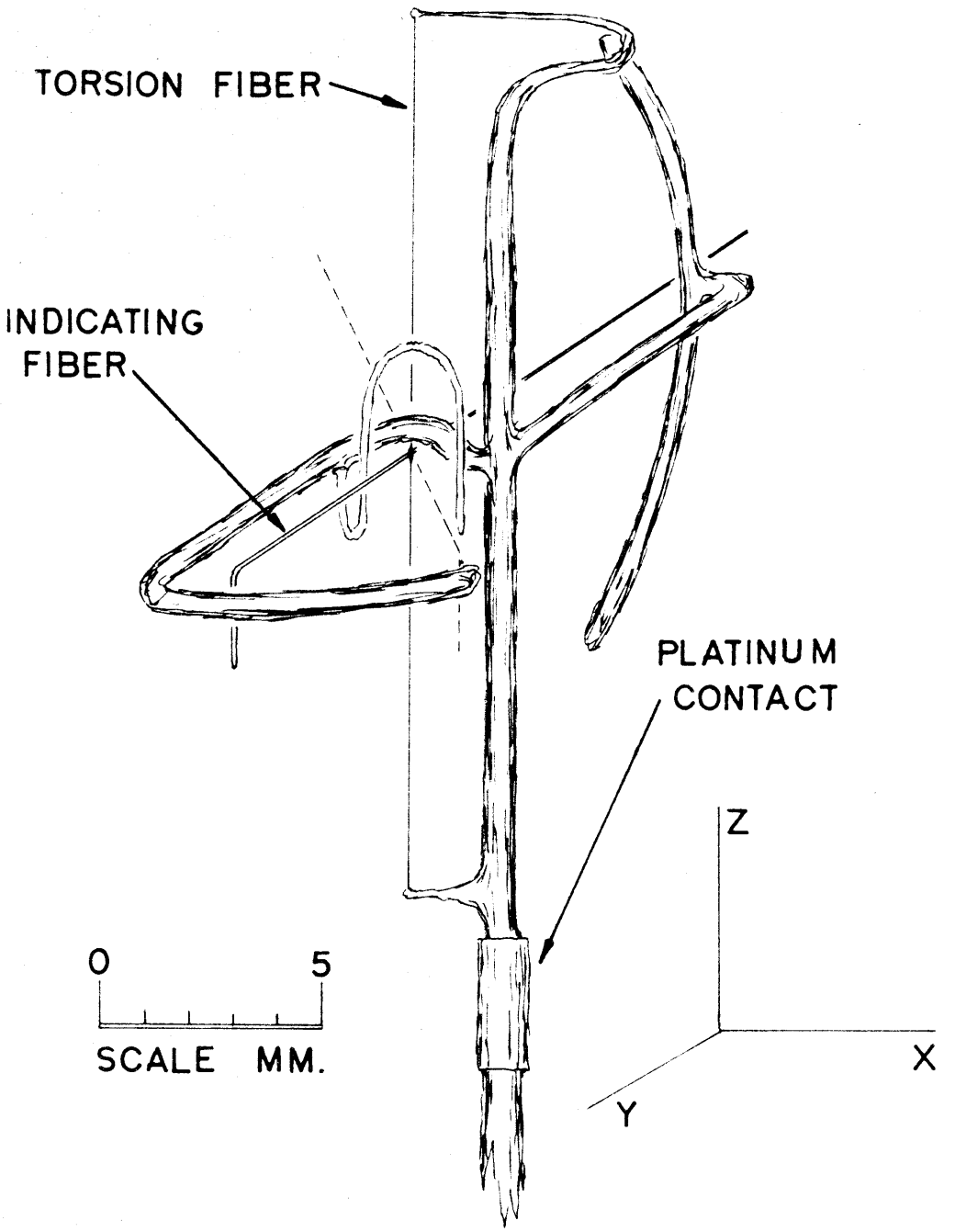

ELECTROSCOPE DESIGN.

NFJ

FIG. 2

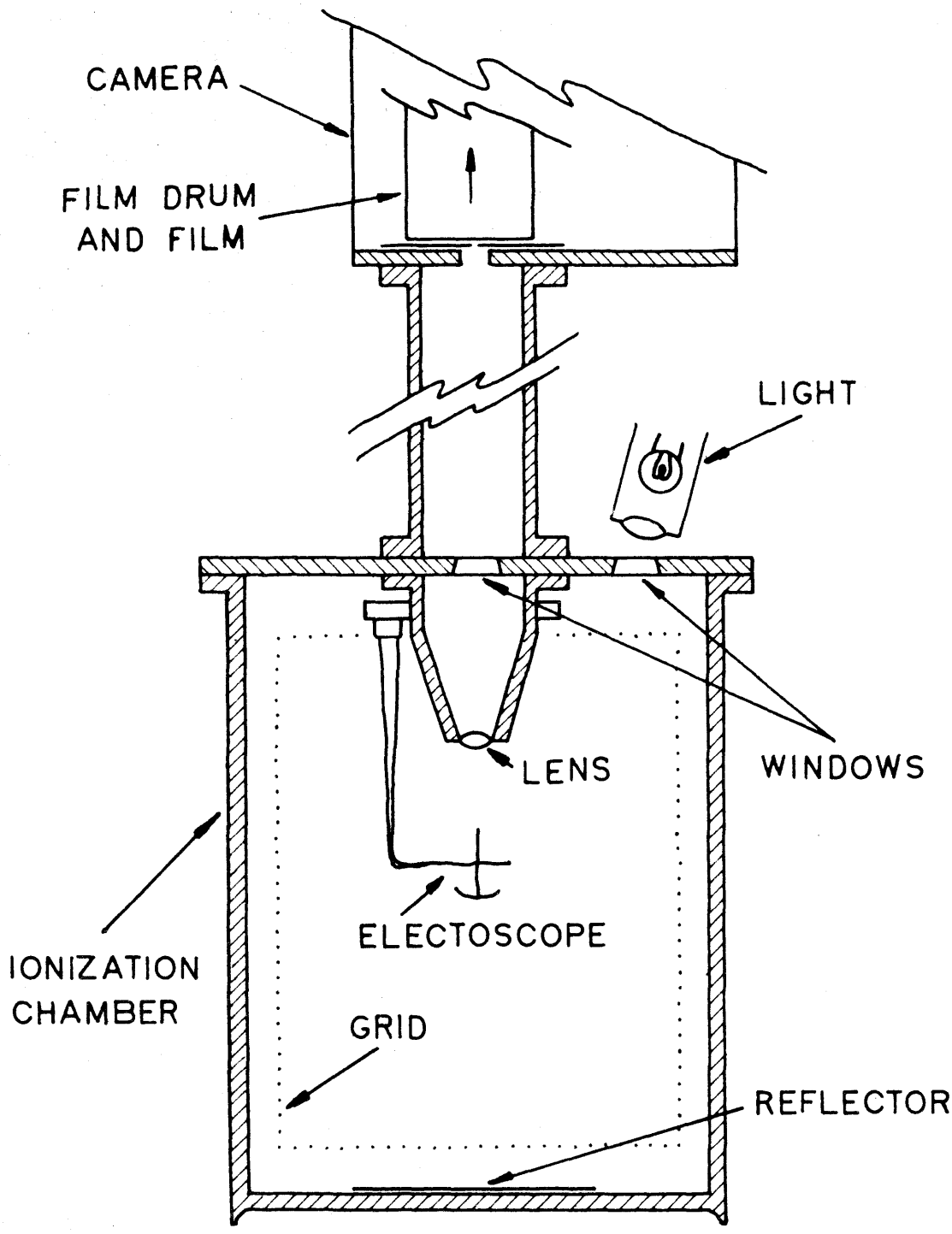

IONIZATION CHAMBER, ELECTROSCOPE AND OPTICAL SYSTEM LAYOUT

NFJ

FIG. 3

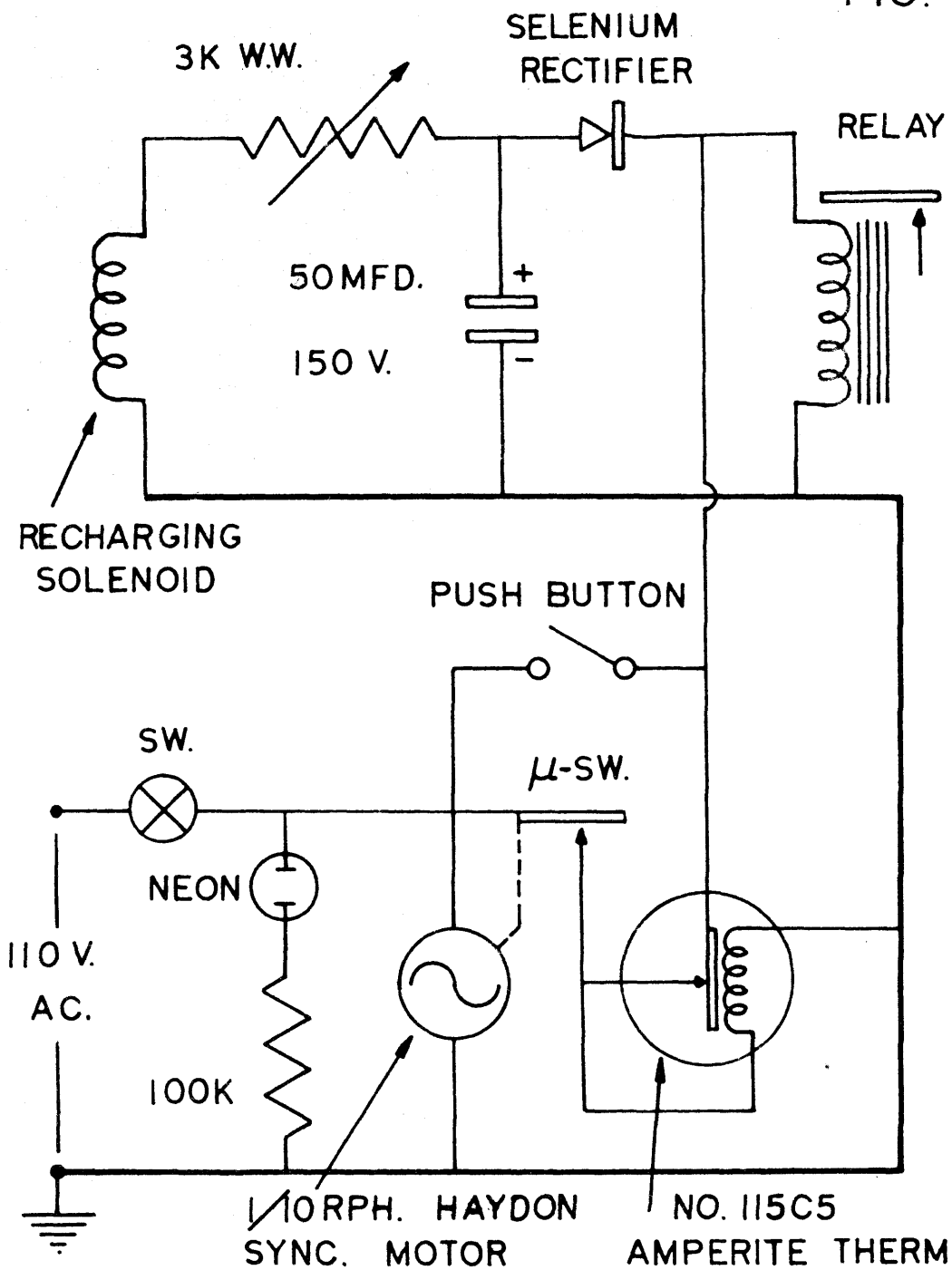

RECHARGING CYCLE - TIMING DEVICE.
(INCLUDING RECHARGING SOLENOID AND RE-CHARGING VOLTAGE RELAY)

NFJ

FIG. 4

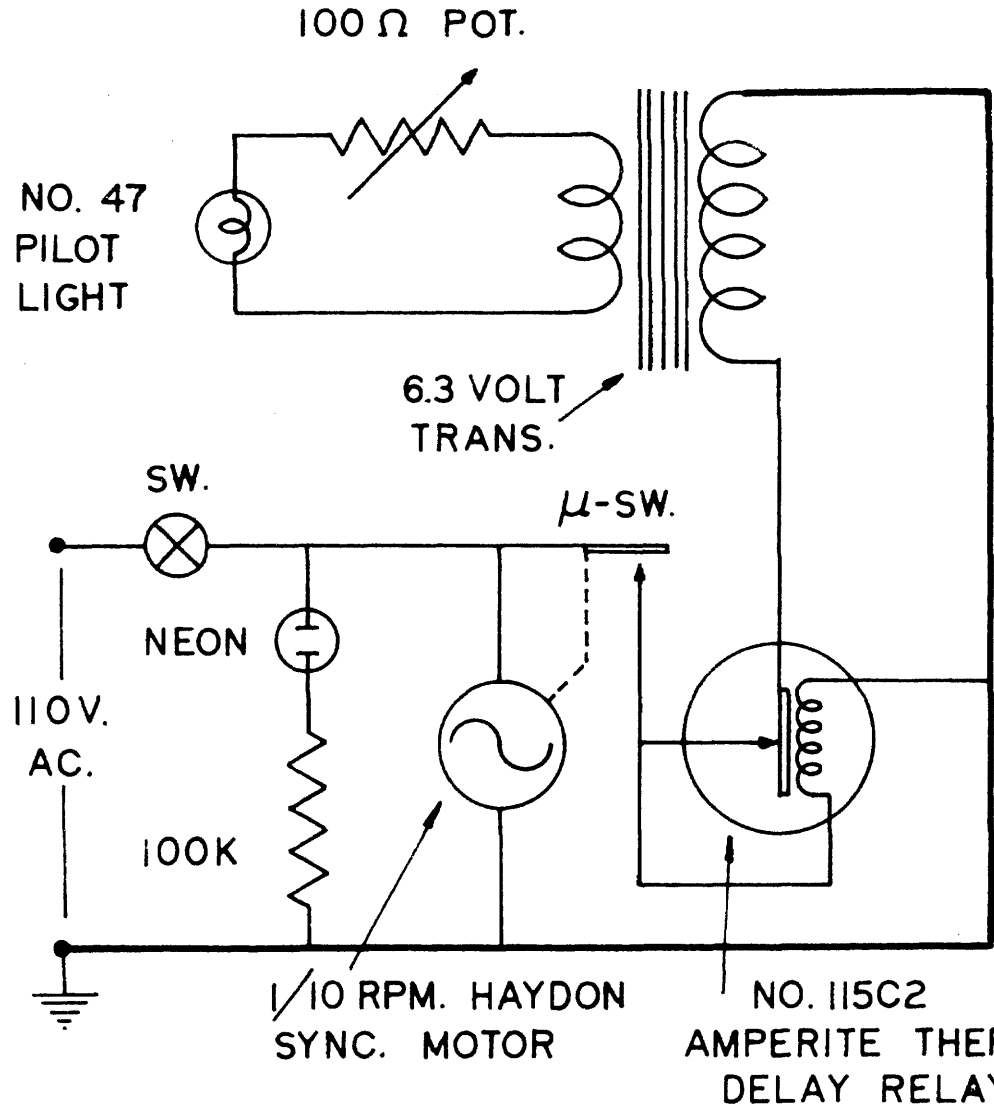

TIME MARKING DEVICE.

BY MEANS OF A CAM MECHANISM, THE MOTOR CLOSES THE μ-SW. EVERY 10 MIN. THIS TURNS THE LIGHT ON, AND THE THERMAL DELAY RELAY ALLOWS IT TO REMAIN ON FOR 2 SEC. THE LIGHT IS LOCATED IN THE OPTICAL TUBE, AND THUS, THE RESULT IS AN IMAGE OF THE SLIT APPEARING ON THE FILM EVERY 10 MIN.

NFJ

FIG. 5

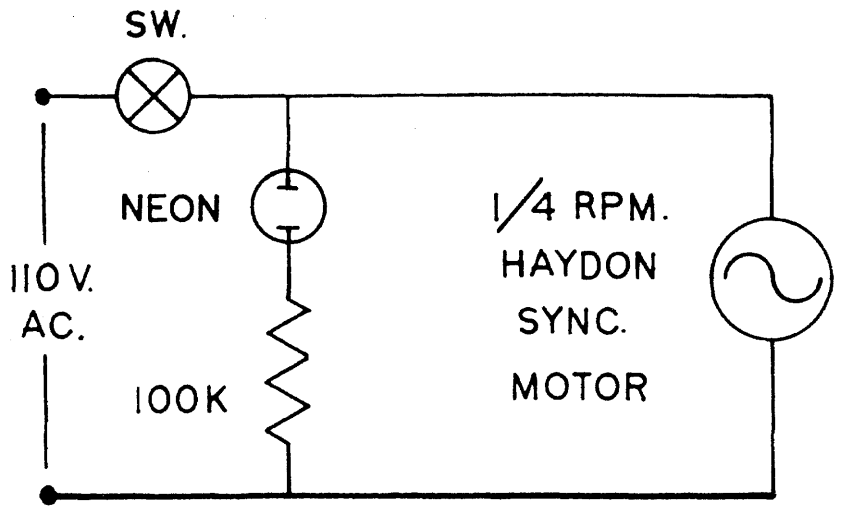

CAMERA - POWER SUPPLY.

FIG. 6

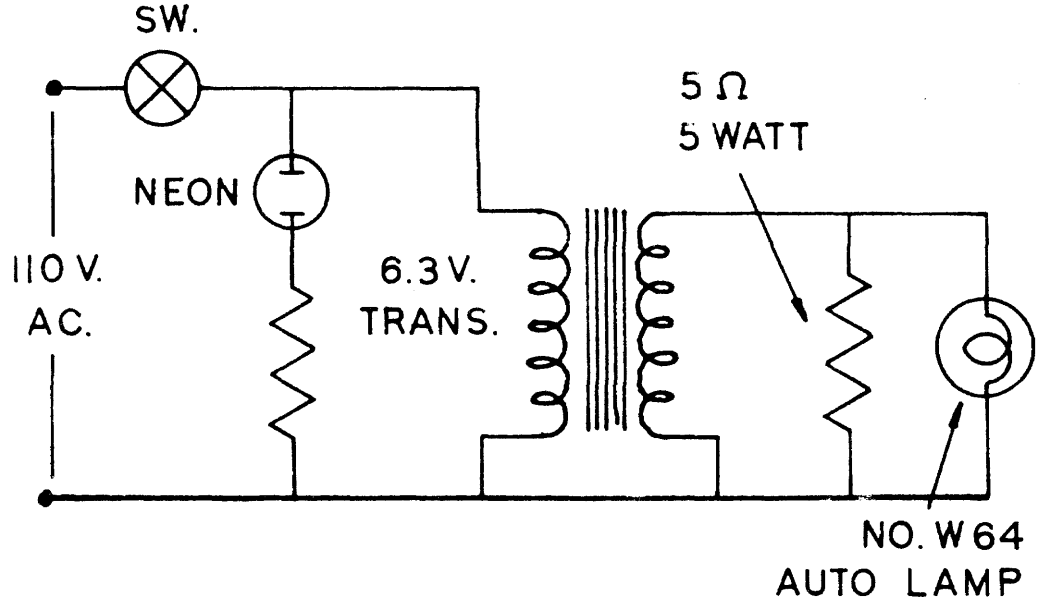

LIGHT SOURCE - POWER SUPPLY.

NFJ

FIG. 7

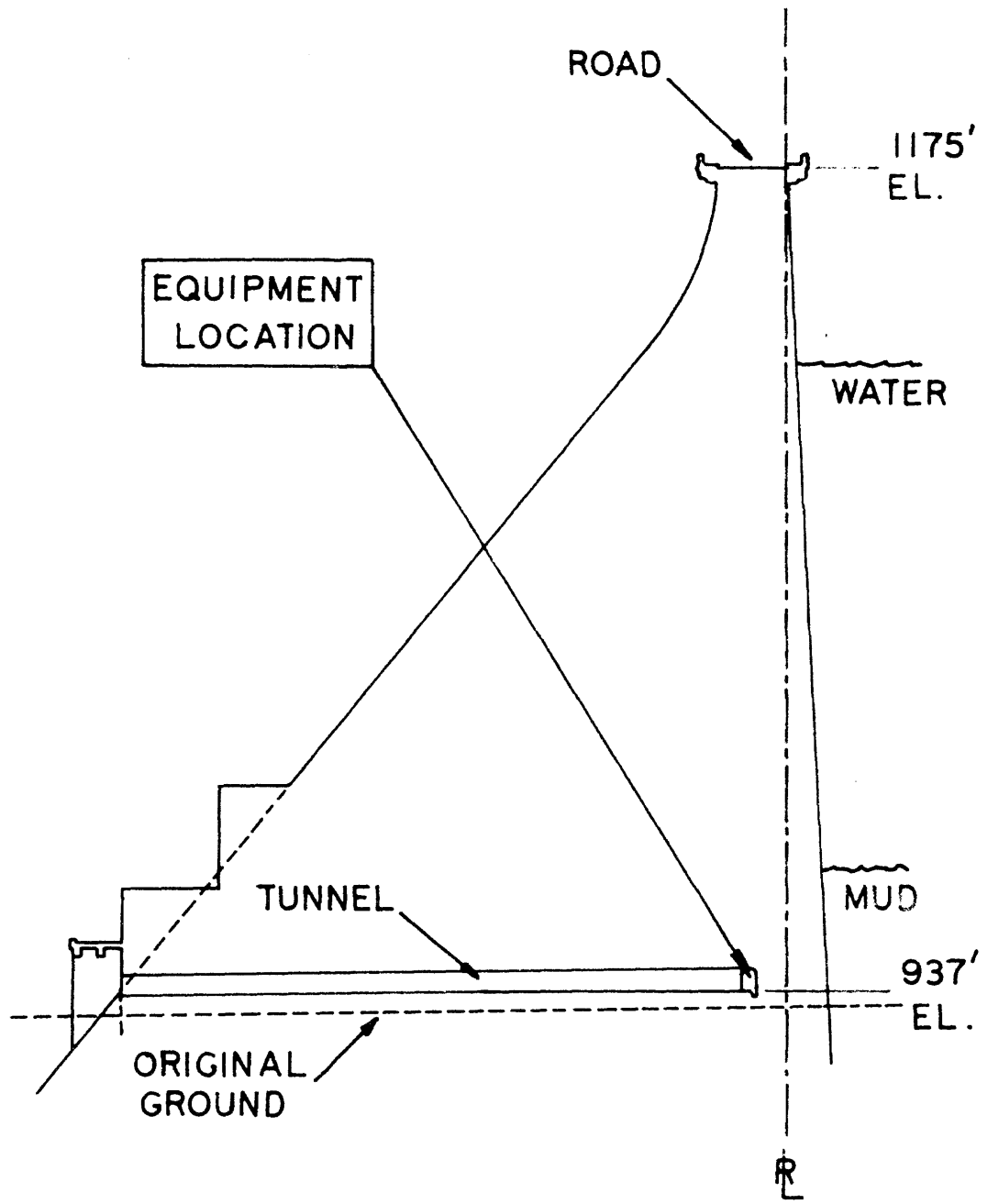

CROSS SECTION OF MORRIS DAM.
(SHOWING LOCATION OF EQUIPMENT)

NFJ

FIG.8

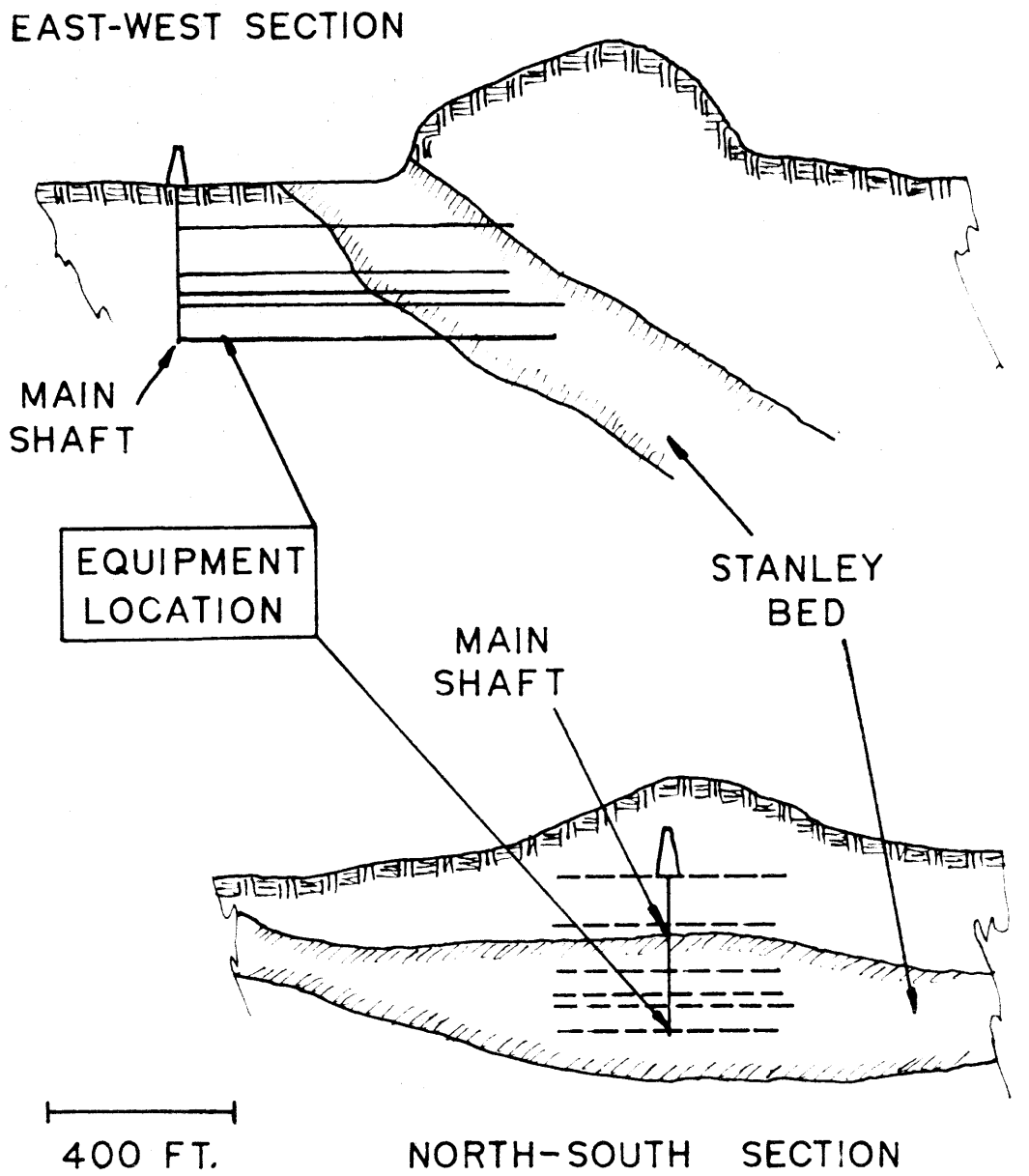

RIVERSIDE CEMENT COMPANY MINE LOCATION

LOCATION DEPTH 325 FT. 267 MWE.

NFJ

FIG. 9

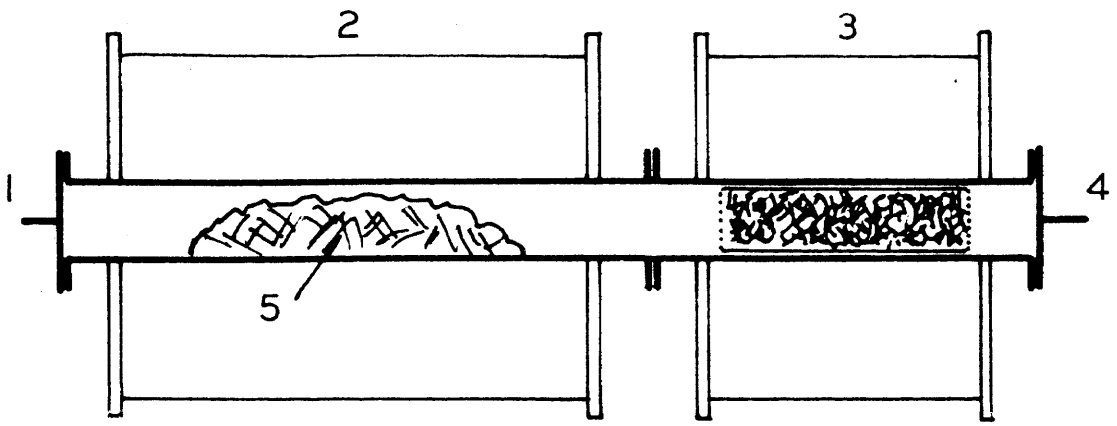

COMBUSTION FURNACE

FIG. 10

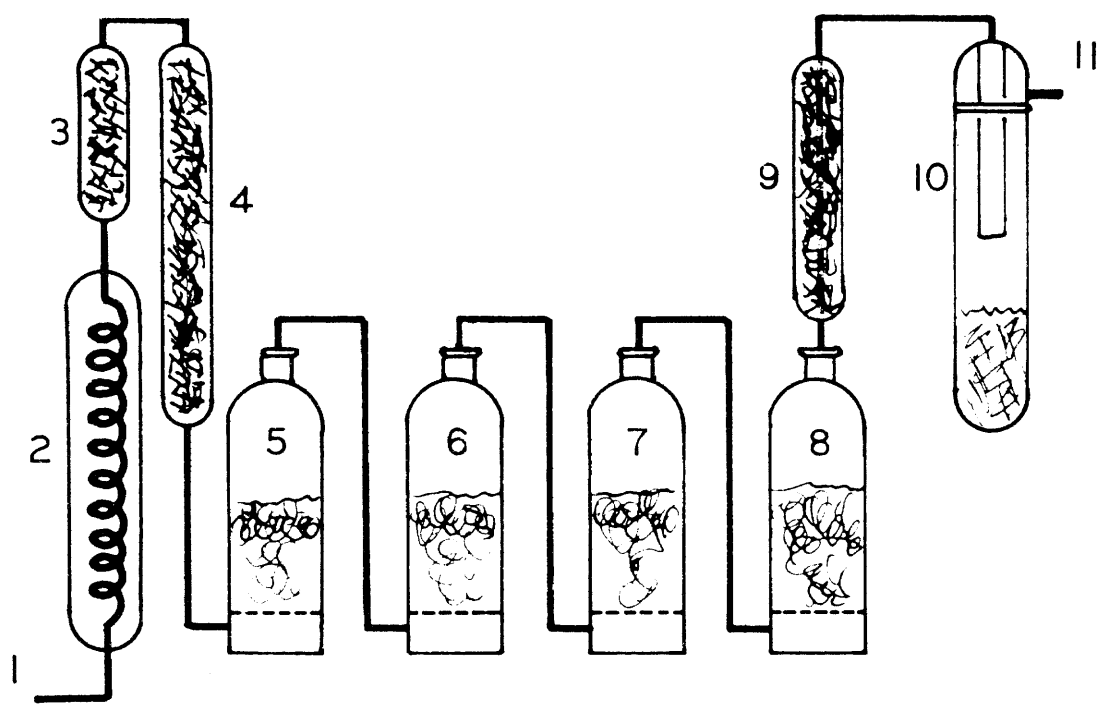

PURIFICATION LINE

NFJ

FIG.11

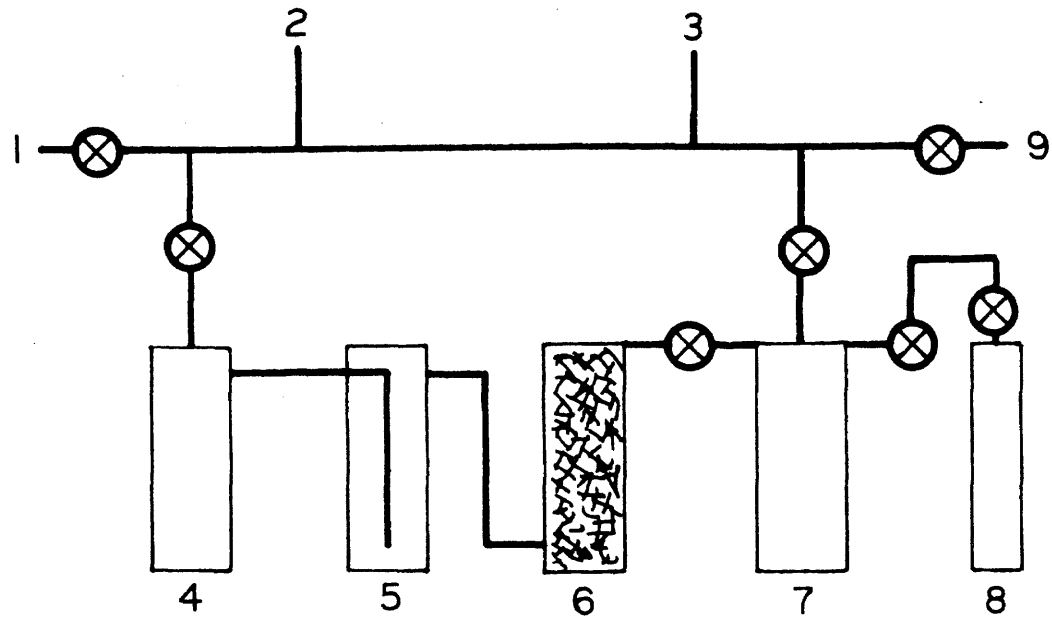

SUBLIMATION SYSTEM

FIG.12

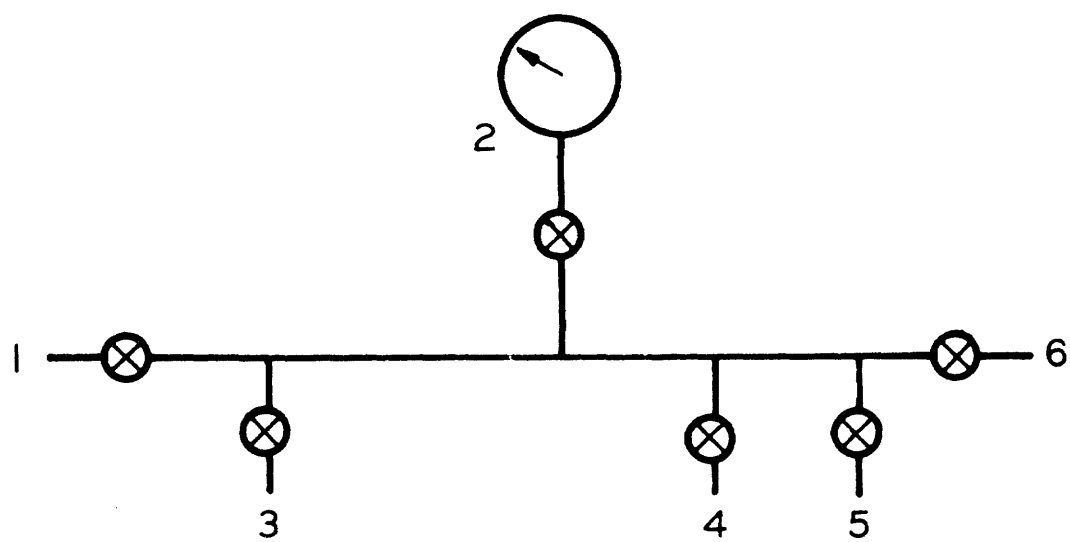

HIGH-PRESSURE SYSTEM

NFJ

Figures:

Figure 1. Electroscope design

This figure is a sketch of the electroscope used in this equipment. The electroscope is constructed of fused quartz with all joints welded; no cements have been used. The torsion fiber has a diameter of approximately 3 microns and the indicating fiber a diameter of approximately 20 microns. The entire system except for a portion approximately 1 cm. long just below the platinum contact is gold plated. The gold plating is done by the vacuum evaporation technique and is approximately 100 Angstroms thick; light easily passes through the gold film. The portion just below the platinum contact which is not gold plated acts as the insulation for the electroscope. This electroscope when placed within the ionization chamber and evacuated to less than 1 micron discharged approximately 100 microns in 24 hours. A deflection of 43 microns per minute represents the discharge rate from normal background radiations. The insulation can be concluded to be satisfactory.

Figure 2. Ionization Chamber, Electroscope and Optical System Layout

This drawing gives the physical relationship of the basic parts of the system. The electroscope is seen mounted in the center of the ionization chamber and grid structure, in front of the observing lens. At the opposite end of the optical tube which is approximately 20 inches long the camera is mounted. The camera system consists of a slit mounted perpendicular to the

indicating fiber and parallel to its motion of travel. The film is mounted on a rotating drum which is just behind the slit. The film travels in a direction perpendicular to the slit and the indicating fibers' direction of motion. The result is a diagonal trace on the film representing time vs. displacement. Since it is very difficult to make the film drum move uniformly, a light was placed in the optical tube and, by means of a time marking device, flashed for 2 seconds every ten minutes. The result is an image or shadow of the slit appearing on the film every ten minutes.

Figure 3. Recharging Cycle-timing Device

Periodically the electroscope must be recharged and this is done by an electromagnetic-mechanical device (see photograph 24) which consists of a recharging arm and energizing solenoid. This figure shows the schematic of the timing device.

Figure 4. Time Marking Device

By means of a cam mechanism operated by a synchronous motor a microswitch is closed every ten minutes, turning on a light. A thermal delay relay allows this light to stay on for approximately two seconds. The light is located in the optical tube of the camera system and the result is an image or shadow of the slit appears on the film every ten minutes.

Figure 5. Camera-Power Supply. A schematic.

Figure 6. Light Source. Power Supply. A schematic.

Figure 7. Cross-section of Morris Dam

This drawing shows the dam in cross section at approxi-

mately the center of the dam. The 937 ft. tunnel is shown and the approximate location of the equipment pointed out.

Figure 8. Riverside Cement Company Mine Location

This drawing shows the east-west and north-south sections of the mine, and the approximate location of the equipment is pointed out.

Figure 9. Combustion Furnace

1. Inlet. A dried mixture of oxygen and neon enters this end of the furnace. The proportions of oxygen and neon are adjustable so that the combustion of the sample may be controlled.

2. Sample combustion furnace. This furnace is operated at from 400 to 500° C. and contains the sample (5) which burns in the controlled atmosphere.

3. Cupric oxide catalytic furnace. This furnace is operated at 300° C. and insures complete oxidation of the sample carbon to carbon dioxide.

4. Outlet. At this point the hot combustion products including the carbon dioxide leave the furnace and enter the purification line.

5. Sample. A typical sample would be of wood or charcoal.

Figure 10. Purification Line

1. Inlet. The hot combustion products from the combustion furnace enter the system here.

2. Cooling condenser. This water cooled condenser cools the hot gases and condenses some impurities such as water

and tar-like combustion products.

3 and 4. Drying tubes. These tubes contain silica gel and are intended to further dry the gases. Two tubes are used because considerable amounts of tar-like substances are collected here, and the first drying tubes allow these substances to drain back into the condenser instead of into the second drying tube.

5. First Scrubber. The first scrubber contains a concentrated chromic acid solution made from 15 cc solution of saturated $Na_2Cr_2O_7$ in 1 liter of concentrated H_2SO_4. This scrubber and the following two contain strong oxidizing solution which oxidize and absorb combustion products other than carbon dioxide which represent impurities.

6 and 7. Second and third Scrubbers. These scrubbers contain identical solutions made from 820 gms $Na_2Cr_2O_7$ $2H_2O$ dissolved in 1 liter of 6.8NH_2SO_4 solution.

8. Fourth Scrubber. This final scrubber contains C.P. concentrated H_2SO_4 and is intended to prevent chromic acid solution carryover as well as partially dry the carbon dioxide.

9. Drying tube. This final drying tube contains calcium chloride and is intended to further dry and filter the carbon dioxide.

10. Receiver. This receiver is maintained at -195° C. with liquid nitrogen, which is below the freezing point of carbon dioxide. The carbon dioxide, which is diluted with helium at

this point, separates out as a snow, dry ice snow. Its appearance is very similar to ordinary snow. After the sample has been completely collected, as indicated by the reduced boiling of the liquid nitrogen as well as the collection of some liquid oxygen, a blue appearing liquid, the receiver is transferred to the sublimation system.

Figure 11. Sublimation System

1. To high-vacuum pumping system.

2. To Pirani-vacuum gage.

3. To inclosed-vacuum gage.

4. First Receiver. The receiver containing the solid carbon dioxide is transferred to the sublimation system at this point; the containers are interchangeable. The carbon dioxide invariably contains oxygen and neon, and consequently, it is pumped on until the pressure drops to less than 1 micron.

5. Trap. This trap is maintained at the melting point of carbon dioxide during the sublimation process. This collects high melting impurities which the carbon dioxide may now contain.

6. Drying tube. This drying tube is packed with magnesium perchlorate and is intended to dry the carbon dioxide to a point satisfactory for ionization chamber use.

7. Second Receiver. This container is maintained at -195° C. with liquid nitrogen during the first sublimation process and thus receives the carbon dioxide. The sample now collects as a single solid since it no longer is diluted.

8. Metal cylinder. After the sample has been sublimed once and again pumped on to insure its freedom from volatile impurities it is resublimed into this metal cylinder. After closing the valve on the metal cylinder it may be allowed to warm to room temperature. The cylinder being capable of withstanding the 900 pounds per square inch, the vapor pressure of the carbon dioxide. The sample is then allowed to age for 30 days, to allow for the decay of radon or thoron, naturally occurring radioactive isotopes of radon, which may have been carried through the purification process.

Figure 12. High-pressure System

1. Connection to vacuum pumping system.

2. High pressure Heise gage. This gage is accurate to one half pound to per square inch from 0 to 300 pounds per square inch.

3. Connection to argon regulator and tank. During preliminary experimental work, the chambers were often filled with argon.

4. Connection to carbon dioxide sample cylinder.

5. Connection to ionization chamber.

6. Connection to outside air pressure.

Experimental Data:

The data given here was obtained at the Morris Dam location.

Preliminary data:

Carbon-14 half-life 5568 ± 30 yrs. (20)

The following is a brief description of each sample of interest which was processed during the course of this work. The samples are numbered according to the cylinder in which they were stored.

Cylinder 1. Sequoia Gigantea redwood--Age 5-105 yrs. This sample was supplied and dated by means of its tree-rings by Professor Edmund Schulman of the University of Arizona, Tucson, Arizona. The average age of the sample is estimated to be 55 ± 2 yrs. and it was used as the modern carbon sample.

Total discharge rate	8.22 ± 0.15(S. D.)$\times 10^{-3}$ cm/min. $\pm 0.9\%$(P. E.)
Sample discharge rate	3.97 ± 0.17(S. D.)$\times 10^{-3}$ cm/min. $\pm 2.9\%$(P. E.)

Cylinder 3. Tank carbon dioxide--Age $> 50,000$ yrs. This sample was taken from a tank of commercial carbon dioxide which originated from the burning of coal and/or petroleum. Previous work with this sample has shown it to be free of contamination and equivalent to a very old carbon sample; this sample was used as the dead carbon sample.

Total discharge rate	4.25 ± 0.08(S. D.)$\times 10^{-3}$ cm/min. $\pm 1.4\%$(P. E.)

Cylinder 4. Gladwin #2997 tree--Age 1835±150 yrs.

This is a sample from the Gladwin collection which was dated by its tree-rings; it is used here as a test of the method.

Total discharge rate	7.26 ± 0.12(S. D.) $\times 10^{-3}$ cm/min. $\mp 1.1\%$(P. E.)
Sample discharge rate	3.01 ∓ 0.14(S. D.) $\times 10^{-3}$ cm/min. $\mp 3.1\%$(P. E.)
Calculated age	2264 ∓ 356(P. E.) yrs.

The tree-ring age and the Calculated age agree within experimental error.

Cylinder 5. Sequoia Gigantea redwood--Age 1455-1502 yrs.

This is another portion of the redwood sample supplied by Professor Edmund Schulman. This sample was also dated by its tree-rings and has an estimated average age of 1489±10 yrs.

Total discharge rate	8.12 ± 0.18(S. D.) $\times 10^{-3}$ cm/min. $\mp 1.5\%$(P. E.)
Sample discharge rate	3.87 ∓ 0.20(S. D.) $\times 10^{-3}$ cm/min. $\mp 3.4\%$(P. E.)
Calculated age	251 ± 360(P. E.) yrs.

The reason for the large discrepancy between the known age and the age as calculated above is not known. The sample is apparently contaminated; however, at what point this occurred is unknown.

Cylinder 6. Sequoia redwood sample. Age 1300±20 yrs.

This is another redwood sample; however, its origin is not known. Its age was determined by its tree-rings.

Total discharge rate	7.60 ± 0.18(S. D.) $\times 10^{-3}$ cm/min. $\mp 1.6\%$(P. E.)
Sample discharge rate	3.35 ∓ 0.20(S. D.) $\times 10^{-3}$ cm/min. $\mp 4.0\%$(P. E.)
Calculated age	1403 ± 396(P. E.) yrs.

The tree-ring age and the calculated age agree within experimental error.

Cylinder 8. La Brea Tar Pits Wood--Age unknown.

This is a wood sample from the La Brea Tar Pits. Previous measurements with similar but different equipment yielded ages of 13,000±2,000 yrs. and 16,300±2,000 yrs.

Total discharge rate	4.74 ± 0.11(S.D.) $\times 10^{-3}$ cm/min. $\pm 1.6\%$(P.E.)
Sample discharge rate	0.49 ± 0.14(S.D.) $\times 10^{-3}$ cm/min. $\pm 19\%$(P.E.)
Calculated age	$16,700 \pm 1,600$(P.E.) yrs.

Cylinder 11. Santa Rosa Island seagrass--Age 3 yrs.

This is a sample of modern seagrass obtained at the Santa Rosa Islands. This sample and those of cylinders 12 and 14 were supplied by Mr. Phil Orr of the Santa Barbara Museum of Natural History, Santa Barbara, California. The significance of this sample and those of cylinders 12 and 14 is discussed at the end of this section.

Total discharge rate	7.78 ± 0.11(S.D.) $\times 10^{-3}$ cm/min. $\pm 0.9\%$(P.E.)
Sample discharge rate	3.53 ± 0.14(S.D.) $\times 10^{-3}$ cm/min. $\pm 2.6\%$(P.E.)
Calculated age	998 ± 315 (P.E.) yrs.

Since this sample is known to be modern, there are at least two possible interpretations of the discrepancy between the known and calculated ages. Either the calculated age is in error, or it is correct, and for some reason the radiocarbon content of seagrass is lower than normal plant life in equilibrium with the carbon reservoir.

Cylinder 12. Santa Rosa Island ancient seagrass--Age unknown.

This Santa Rosa Island sample is of unknown age; however, its

estimated age is roughly 400 yrs. based on archeological evidence. The Santa Barbara Museum of Natural History designation for this sample is:

131.2 T-4, Skull Gulch, seagrass (on cliff face)

Obtained Nov. '52.

Total discharge rate	7.59 ± 0.12(S. D.) $\times 10^{-3}$ cm/min. $\mp 1.1\%$(P. E.)
Sample discharge rate	3.34 ∓ 0.14(S. D.) $\times 10^{-3}$ cm/min. $\mp 2.9\%$(P. E.)
Calculated age	1425 ∓ 330(P. E.) yrs. 437 ∓ 311(P. E.) yrs.

Two different ages are given here depending on what value is taken for the modern carbon discharge rate. If one uses the sample of cylinder 1, the 1425 yrs. age is obtained. If one uses the sample of cylinder 11, the 437 yrs. age is obtained. Since the latter value agrees with the archeological estimate, it would seem to be the most likely value.

Cylinder 14. Santa Rosa Island ancient charcoal--Age unknown.

The estimated age of this sample is greater than 4,000 yrs. and as with the sample of cylinder 12 is based on archeological evidence. The Santa Barbara Museum of Natural History designation for this sample is:

131.4 Arlington dune, charcoal (Sweat House).

Obtained Nov. '52.

Total discharge rate	7.03 ± 0.13(S. D.) $\times 10^{-3}$ cm/min. $\mp 1.3\%$(P. E.)
Sample discharge rate	2.88 ∓ 0.15(S. D.) $\times 10^{-3}$ cm/min. $\mp 3.6\%$(P. E.)
Calculated age	2620 ∓ 365 (P. E.) yrs.

In order to give some understanding of the significance of the Santa Rosa Island samples, a sketch of the archeology of the Santa Rosa Islands and its relation to the carbon-14 dating will be included here. It was obtained from Mr. Orr of the Santa Barbara Museum of Natural History.

Sketch of the Archeology of Santa Rosa Island in Relation to Carbon-14 Dating

No carbon-14 dates are available for any southern California site. Yet, southern California is probably one of the richest archeological areas in the country, and the Santa Rosa Islands offer the best opportunity to study the archeology undisturbed. On the mainland, most of the sites have been disturbed by pot hunters, early expeditions or commercial activity, but on the islands, there is relatively virgin territory, which the Santa Barbara Museum of Natural History has been exploring for the past eight years.

Geologic and Archeologic History:

During the pleistocene, the islands were connected to the mainland, and mammoth, mice, fox and skunk were isolated when the land connection was broken. This resulted in different species or subspecies developing and in the eventual extinction of the mammoth.

The climate was cold and wet; forests covered the islands, and streams ran into the sea, creating a delta at the mouth of each stream and depositing mammoth bones, wood and charcoal in these beds.

Samples of charcoal from the bottom of the mammoth beds, and shells from the top of the beds are available for Carbon-14 dating, and it would be extremely interesting to know just what the date of the existence and extinction of the mammoth was. This animal, Archidiskodon exilis, was described by Stock and Furlong of the California Institute of Technology; a skull is on display at the California Institute of Technology Museum, others at the Santa Barbara Museum of Natural History.

About the time of the extinction of the mammoth, man arrived on the island, and human remains and mammoth bones are found within six inches of each other in the strata. The first men lived about ponds, and subsequent deposition has covered his camp sites with approximately six to eight feet of water-laid sediments.

With the change from wet to dry, the ocean began to erode into the shoreline, and thus increased the fall of the streams, making eventually high sea cliffs and deep gorges. On the land, huge sand dunes built up a quarter to one-half mile inland and covered over Indian villages, but the people continued to live in the vicinity so that their middens are contained in layers in the sand dunes. Thirty feet of windblown material covers some of these sites. These people's culture we know as the Dune Dweller culture.

Again the climate turned wet, and trees and bushes grew on the sand dunes; their root casts are to be seen today. Heavy rainfall created forests on the highlands, ponds and streams; and a new culture appears which lived on these highlands, well back from the ocean. We know very little about this culture as our excavations for the past six years have concentrated upon the earlier Dune Dwellers and the later Canalino culture.

The Canalinos appeared after the climate had again changed to dry; the forests disappeared, and they lived on the seacoast, utilizing fish as their main source of food. This was the group of Indians which inhabited the island and the adjacent mainland at the time of the white man's first contact in 1542.

A fourth group of people are found on the island, but we are unable, as yet, to place them in the chronology. These are the cave dwellers, who occupied shallow caves for a long period of time prior to the second wet period, but whether they came before the Dune Dwellers or later has not been determined.

Value of Carbon-14 Dating:

From the geological and paleontological point of view, it is very desirable to have dating on the mammoth period, either the earliest (charcoal)

or latest (shell) or both. This will also give a time for the first wet period, which quite probably corresponds to the pluvial period of Lake Lahontan and Bonneville. Inasmuch as the shell, mentioned above, is evidence of man, this should give us the earliest date for man on the island, and thus, so far as we know, the approximate earliest date for man in California.

A series of dates during the occupation by man is very desirable, as it will tell us not only when various groups appeared or disappeared, but will also tell us a good deal about the time when the climate changed on the island, and by inference, when it changed on the mainland. Similar conditions occur on the mainland, but it is not as simple to study them and to collect samples as on the island.

Furthermore, inasmuch as the islanders supplied the bulk of shell ornaments for the rest of the state, Nevada and Arizona, by dating these various objects at their source, sites in the interior can be dated by their artifact content.

Chronology of Santa Rosa Cultures:

Climate	Culture	Period	Phase	Years BP
	Caucasian	Modern	Historical contact	150 to 500
Dry	Canalino	LATE	late interm early	 437 1425 (?)
Wet	Highlander	INTERMED	late interm. early	
	Cave (?)			
Dry	Dune Dweller	EARLY	late interm. early	2600 (?)
	Cave (?)			
Wet	Mammoth	Pleistocene		

REFERENCES

(1) A. V. Grosse, "An Unknown Radioactivity", J. Amer. Chem. Soc., 56 1922 (1934).

(2) S. A. Korff, "On the Contribution to the Ionization at Sea-level Produced by the Neutrons in the Cosmic Radiations", Terr. Mdg. and Atm. Elec., 45 133 (1940).

(3) W. F. Libby, "Atmospheric Helium 3 and Radiocarbon from Cosmic Radiation", Phy. Rev., 69 671 (1946).

(4) C. E. Anderson, W. F. Libby, S. Weinhouse, A. F. Reid, A. D. Kirshenbaum and A. V. Grosse, "Radiocarbon from Cosmic Radiation", Science, 105 576 (1947).

(5) C. E. Anderson, W. F. Libby, S. Weinhouse, A. F. Reid, A. D. Kirshenbaum and A. V. Grosse, "Natural Radiocarbon from Cosmic Radiation", Phy. Rev., 72 931 (1947).

(6) C. E. Anderson, J. R. Arnold and W. F. Libby, Rev. Sci. Inst., 22 225-32 (1951).

(7) J. L. Kulp and L. E. Tyron, "Extension of the Carbon-14 Age Method", Rev. Sci. Inst., 23 296 (1952).

(8) H. R. Crane, "Dating of Relics by Radiocarbon Analysis", Nucleonics, 9 16 (1951).

(9) A. R. Crathorn, "Use of an Acetylene-filled Counter for Natural Radiocarbon", Nature, 172 632-3 (1953).

(10) W. A. Burke and W. G. Weinschein, "Carbon-14 Dating with a Methane Proportional Counter", Rev. Sci. Inst., 26 1137-40 (1955).

(11) E. Broda, "Geiger Counting of Carbon Dioxide", J. Inorg. and Nucl. Chem., 1 411-72 (1955).

(12) G. L. Fergusson, "Radiocarbon Dating System", Nucleonics 13 (No. 1) p. 18 (1955).

(13) J. R. Arnold,"Scintillation Counting of Natural Radiocarbon: I The Counting Method", Science, 119 155 (1954).

(14) John Strong, "Procedures in Experimental Physics", Prentice-Hall, Inc., (1938), Ch. V, p. 188.

(15) E. Segre (Editor), "Experimental Nuclear Physics", John Wiley and Sons, (1953), p. 238.

(16) J. A. Beardon, "Radioactive Contamination of Ionization Chamber Materials", Rev. Sci. Inst., 4 271 (1933).

(17) D. L. Douglas, Thesis - California Institute of Technology, 1950.

(18) M. Shein and P. S. Gill, "Burst Frequency as a Function of Energy", Rev. Mod. Phy. 11 267 (1939).

(19) V. C. Wilson, "Cosmic Ray Intensity at Great Depths", Phy. Rev., 53 337 (1938).

(20) J. R. Arnold and W. F. Libby, "Radiocarbon Dates", Science, 113 111-120 (1951).

(21) G. Freidlander and J. W. Kennedy, "Introduction to Radiochemistry", John Wiley and Sons, (1949), p. 206.

The Beta Energy Spectrum's Effect on the Statistics of Measurement of an Ionization Chamber.

For the sake of comparison, consider two measuring devices of exactly the same sensitive volume and containing exactly the same size gaseous sample of a carbon-14 containing substance. Specifically, consider a G.M. counting tube such as used by Libby and a current ionization chamber such as described in this thesis. In the case of the G.M. tube every beta particle, regardless of energy, will produce a recordable count. The statistics of such a system have already been worked out (21), and show that the accuracy of any given measurement is as follows:

$$N \pm \sqrt{N} \quad \text{(Standard deviation)}$$

where N is the number of counts observed. If these N counts were observed over a period of time, T, the rate is:

$$\frac{N}{T} \pm \frac{\sqrt{N}}{T} \quad \text{(Standard deviation)}$$

In the case of the ionization chamber, every beta particle, regardless of energy, will also be observed by means of the ion current it produces. The magnitude of this ion current, I, can be expressed as follows:

$$I = \frac{NE_{ave}}{e_T}$$

where N is the number of beta particles, E_{ave} is the average beta energy and e is the average energy required per ion-pair.

If the beta spectrum is a delta function at E_{ave}, the result is:

$$I = \frac{N E_{ave}}{e_T} \pm \frac{E_{ave}}{e_T} \sqrt{N} \qquad \text{(Standard deviation)}$$

If the beta spectrum consists of two delta functions at $2E_{ave}-\Delta E$ and ΔE, the result is:

$$I = \frac{N}{2} \cdot \frac{2E_{ave}-\Delta E}{e_T} + \frac{N}{2} \frac{2(\Delta E)}{e_T}$$

$$\pm \left[\left(\frac{2E_{ave}-\Delta E}{e_T} \right)^2 + \left(\frac{2\Delta E}{e_T} \right)^2 \right]^{\frac{1}{2}} \left(\frac{N}{2}\right)^{\frac{1}{2}}$$

If ΔE is allowed to go to zero, the results become:

$$I = \frac{NE_{ave}}{e_T} \pm 1.41 \frac{E_{ave}}{e_T} \sqrt{N} \qquad \text{(Standard deviation)}$$

The standard deviation is, therefore, 41% worse than for the G. M. tube. Considering a more realistic spectrum, one finds that for a rectangular spectrum the statistics are 16% worse, and for a triangular spectrum the statistics are 22% worse. Considering an actual spectrum, one would expect the statistics to be from 20 - 25% worse.

PROPOSITIONS

1. In the paper entitled "The Nature of Statistical Fluctuations with Applications to Cosmic Rays" by R. D. Evans and H. V. Neher (1), it is stated that the statistics concerning a differential system are essentially $2^{1/2}$ times worse than with a simple system. It is proposed that this conclusion is in error due to the experimental design which was assumed. It is further proposed that assuming the proper design it can be shown that the statistics are essentially equivalent to those of a simple system.

2. Although it is not commonly known, there is reasonable evidence that the accepted value for the half-life of carbon-14 is in error (2). It is suggested that an additional determination of the half-life would be worthwhile using a different type of system. The proposed system would be a grid-walled ionization chamber with the carbon-14 being contained in the filling gas. It is further proposed that measurements be made at different filling gas pressures such that the data may be extrapolated to infinite pressure thus eliminating the wall effects.

3. As indicated in this thesis, the problem of material contamination is a real one. With the recent introduction of the atomic bomb and the nuclear pile, the possibility of such contamination becomes greater. Consequently, it is proposed that the scientific world acknowledge this and take steps to prevent the possible consequences. As one phase of this preventive action,

it is suggested that facilities be established to produce radiochemically purified materials for use in various types of equipment, for example, low level radiation detection equipment.

4. It has recently been reported (3) that Ta-180 exists in nature and has a relative abundance of 0.0123%. It is proposed that this isotope is radioactive with a half-life that will account for its low relative abundance. It is also proposed that Pt-190 (rel. abund. 0.012%) and Os-154 (rel. abund. 0.018%) are also radioactive with half-lives which account for their low relative abundances. The predicted half-lives for these isotopes would be on the order of 5×10^8 yrs.

5. V-50, which is apparently a stable isotope (rel. abund. 0.24%), must be unstable due to the existence of the stable isobars Ti-50 and Cr-50. It is proposed that the instability may possibly be detected by means of a neutron activation analysis experiment making use of the reaction $Cr^{50}(n, r)\ Cr^{51}$.

6. The practical uses of radioactivity and the nuclear radiations therefrom depends greatly on the ruggedness and reliability of the radiation detection system. In most cases, the weaknesses are due to the critical operating conditions of the sensing element and the lack of reliability of the associated electronics. It is proposed that the combination of the rugged ionization chamber and the reliable magnetic amplifier is worthy of consideration. It

is believed that the design problems can be overcome and that the resulting device would be well worth its development.

7. Reactions between gaseous molecule ions and gaseous molecules have been reported (4). It is proposed that such reactions may be useful in the preparation of small quantities of high specific activity, tagged compounds.

8. Positive evidence has been reported for natural occurrence of Tc-98 (5). It is proposed that the evidence, contrary to their opinion, is more easily explained by not assuming the existence of the Tc-98 isotope.

9. It is difficult to construct a mechanical system which will rotate a drum or wheel at a very low and very uniform rate. Often eccentricities in gears cause rate variations, and frictional forces coupled with the backlash in the system cause a stop-and-start type of motion. It is proposed that a possible solution may be obtained by the use of a differential. The differential would be driven from both ends in different directions at relatively high but slightly different rates; the carriage would then rotate at the difference speed.

10. An effect has been observed where by a soft beta emitting source which is mounted within an ionization chamber can

be "turned on and off" by means of an electric potential which is applied to the source holder. It has also been observed that the degree with which the source is turned on or off depends critically on the potential difference between the source holder and the chamber wall. This effect possibly has application as a voltage comparison device which would be relatively independent of ambient conditions.

REFERENCES

(1) R. D. Evans and H. V. Neher, Phy. Rev., 45 144 (1934).

(2) R. S. Caswell, J. N. Brabant and A. Schwebel, Jour. Res. N.B.S., 53 27 (1954).

(3) F. A. White, T. L. Collins and F. M. Rourke, Phy. Rev., 97 566 (1954).

(4) D. O. Schissler and D. P. Stevenson, Jour. Chem. Phys., 24 926 (1956).

(5) E. Anders, R. N. Sen Sarma and P. H. Kato, Jour. Chem. Phy., 24 622 (1956).